Self-regulation of Anterior Insula Using Real-time fMRI and Behavioral Effects in Obsessive Compulsive Disorder

Dissertation

zur Erlangung des Grades eines

Doktors der Naturwissenschaften

der Mathematisch-Naturwissenschaftlichen Fakultät

und

der Medizinischen Fakultät

der Eberhard-Karls-Universität Tübingen

vorgelegt

von

Korhan Buyukturkoglu

aus Ankara, Türkei.

August - 2014

Tag der mündlichen Prüfung:	26.09.2014
Dekan der Math.-Nat. Fakultät:	Prof. Dr. W. Rosenstiel
Dekan der Medizinischen Fakultät:	Prof. Dr. I. B. Autenrieth
1. Berichterstatter:	Prof. Dr. Niels Birbaumer
2. Berichterstatter:	Prof. Dr. Christoph Braun
Prüfungskommission:	Prof. Dr. Niels Birbaumer
	Prof. Dr. Christoph Braun
	Prof. Dr. Tilo Kircher
	Prof. Dr. Cornelia Herbert

I hereby declare that I have produced the work entitled: “Self-regulation of Anterior Insula Using Real-time fMRI and Behavioral Effects in Obsessive-Compulsive Disorder”, submitted for the award of a doctorate, on my own (without external help), have used only the sources and aids indicated and have marked passages included from other works, whether verbatim or in content, as such. I swear upon oath that these statements are true and that I have not concealed anything. I am aware that making a false declaration under oath is punishable by a term of imprisonment of up to three years or by a fine.

Tübingen, ______________ __________________

Date Signature

Table of Contents

ACKNOWLEDGEMENTS

First of all, I would like to thank my supervisor, Niels Birbaumer for giving me the opportunity to work in his lab, for his ideas and his generous support.

Secondly, I would like to thank Ranganatha Sitaram for his supervision, for his belief in my schemes and for his magnificent contributions to my work. Throughout the past three incredible years, he was always with me with his ideas, experience and support. During my studies either in United States or in Germany, I always considered him as a member of my family. I will never forget my first day in the MPI when we met for the first time; that was a turning point in my life.

I heartily thank to Ozge Yilmaz. She supported me like my sister since the beginning.

I am grateful to Sergio Ruiz and Jens Sommer for their friendship, collaboration and help. I have learnt so much from them.

I thank Prof. Tilo Kircher for giving me the tools and conditions necessary to manifest this work at the Dept. Of Psychiatry, University of Marburg.

I thank Prof. Christoph Braun for his help and advice.

I thank Dr. Nazli Hayirli for her friendship and help in every context especially in infuriating MS Office problems.

I thank members of my lovely music band "Call me Heike", namely, Colleen Dockery, Kristina Führ, Eva Rollbuehler and Fabian Griese for the beautiful music that we played/recorded together.

Also, I thank to my dear friends and colleagues, Ander Ramos, Mohit Rana, Kerstin Mayer, Eliana Garcia, Lilian Konicar, Rahim Malekshahi, Nadine Simon, Leonie Dietzsch, Ezgi Arikan, Andreas Schmidt, Chiara Fioravanti, Aniruddh Ravindran, Niraj Lodaya and Enrico Opri a.k.a. Ginko Biloba, for their friendship and for the wonderful times that we have spent together.

At the end I would like to thank my *family*; my beautiful, precious *family*. We missed each other so much. Now its time to reunite…

List of Abbreviations

BCI	Brain-Computer Interface
BDI	Beck Depression Inventory
BOLD	Blood Oxygenation Level Dependent
EDT	Ecological Disgust Test
EEG	Electroencephalography
FEE	Fragebogen zur Erfassung der Ekelempfindlichkeit
FNIRS	Functional Near Infrared Spectroscopy
HR	Heart Rate
MoCo	Motion Correction
MWI	Mehrfachwahl-Wortschatz-Intelligenztest
OCD	Obsessive-Compulsive Disorder
OFC	Orbitofrontal Cortex
RtfMRI	Real-time Functional Magnetic Resonance Imaging
SCID-I	Structured Clinical Interview for DSM-IV Axis I Disorders
SCR	Skin Conductance Response
STAI	State-Trait Anxiety Inventory
TBV	Turbo BrainVoyager
TR	Repetition Time
YBOCs	Yale-Brown Obsessive Compulsive Scale
SPM	Statistical Parametric Mapping

To my *“family”*

Self-regulation of Anterior Insula Using Real-time fMRI and Behavioral Effects in Obsessive-Compulsive Disorder

2. Introduction

2.1. Obsessive-compulsive disorder, disgust feeling and anterior insula

Obsessive-compulsive disorder (OCD) is a common, chronic condition that can have disabling effects on both genders throughout the patient's lifespan. It is among the most disabling anxiety conditions and accounts for more than half of serious anxiety cases (Ruscio, Stein, Chiu, & Kessler 2010). To be diagnosed with OCD, a person must have obsessions and/or compulsions (DSM-IV-TR, 2000). Among the most common obsessions are contamination fears (usually followed by washing compulsions), which are intense and intrusive feelings of being polluted or infected by contact with the dirty, infectious or soiled objects (Rachman, 2004; Broderick, Grisham & Weidmann, 2013).

The exploration of the neural basis of OCD with functional magnetic resonance imaging (fMRI) has revealed an abnormal activation of several brain areas including the prefrontal cortex, orbitofrontal cortex, cingulate gyrus, thalamus, putamen and globus pallidus (Millet et al., 2013). Hence, current models of the disease hypothesize a dysfunction in the cortico-subcortical circuitry (Aouizerate et al., 2004; Menzies et al., 2008). More recent efforts have tried to elucidate its neural basis in concordance with the heterogenic symptomatology of the disorder.

Several studies have shown a link between contamination fears, disgust over-reactivity and insula activation. Although, activation in the insula is associated with many interoceptive/subjective feelings (e.g., pain, temperature, or itch stimuli) the anterior part of this paralimbic structure is involved in disgust processing as a part of the gustatory cortex, containing neurons that respond to pleasant and unpleasant taste (Craig, 2011; Wright et al., 2004; Rolls, 1994).

Several sources of evidence support the aforementioned link between contamination fears, disgust over-reactivity and anterior insula. First, disgust, which might be triggered by actual or perceived threat of contamination with the objects considered to be unclean, infectious or corrupted, is strongly associated with the fear of contamination and subsequent washing compulsions (Broderick, Grisham & Weidmann, 2013; Olatunji et al., 2004; Stein et al., 2006). Furthermore, heightened disgust feelings towards disgust-inducing stimuli and greater behavioral avoidance from disgusting objects, situations and places are commonly observed in OCD patients, especially those with contamination fears and washing compulsions (Starcevic et al., 2013, Olantunji et al., 2007, Tsao & McKay, 2004; Cisler et. al, 2009; Muris et. al, 2008; Schienle et. al, 2003; Phillips et al., 2000; Sieg and Scholz, 2001: Moretz et al., 2008; Goetz et al., 2013). On the other hand, findings from functional neuroimaging studies (including fMRI and positron emission tomography-PET) have indicated that, when subjects are presented with disgust inducing stimuli, the insula is easily activated in persons with OCD, especially in the group of patients with contamination fears (Phillips, 2000; Shapira, 2003; Mataix-Cols et al., 2004; Stein et al., 2006).

Considering this evidence, it is possible to state that an over-activation in the anterior part of the insular cortex, and disgust over-reactivity could contribute to avoidance and ritualistic behaviors by increasing the aversiveness of exposure to certain stimuli, and strengthening beliefs about contamination (Berle & Phillips, 2006). These results suggest that a reduction of insula activity should enable a reduction in contamination anxiety in the subgroup of OCD patients with predominantly contamination fears and washing compulsions.

2.2. Brain-computer interfaces (BCIs) and their usage in OCD

Brain-Computer Interfaces (BCIs) utilize neurophysiological brain signals to activate or deactivate external devices or computers (Birbaumer & Cohen, 2007). With the introduction of real-time functional magnetic resonance imaging (rtfMRI), voluntary control over specific brain areas was achieved with rtfMRI neurofeedback both in healthy participants (e.g., Caria et al., 2007, 2010; Veit et al., 2012, Sitaram et al., 2010) and people suffering from neuropsychiatric diseases, such as schizophrenia and depression (e.g., Sitaram, 2008a;

Sitaram et al., 2012; Ruiz et al., 2013; Linden et al., 2012). (For detailed reviews see Birbaumer et al., 2013; Ruiz et al., 2013; Sulzer et al., 2013).

In a recent study, Scheinost and colleagues (2013) explored the effect of rtfMRI neurofeedback training on healthy individuals without a clinical diagnosis of anxiety disorder, but who suffered from contamination anxiety. Participants who successfully learned to control the activity of orbitofrontal cortex in the presence of disgust inducing stimuli, displayed changes in resting-state connectivity across different brain areas and an enhanced control over contamination anxiety many days after the completion the training. These results encourage the application of rtfMRI neurofeedback in OCD patients.

3. Aims of the project

In the light of these findings, to choose optimal clinical, behavioral and physiological parameters for a future larger rtfMRI study with group data, we designed a pilot case series study in OCD patients (3 adult patients-2 female) diagnosed by a standardized clinical interview as having contamination obsessions and washing compulsions. Patients were recruited from the Department of Psychiatry and Psychotherapy, University of Marburg.

Our study had three major aims. Our first aim was to explore whether patients suffering from OCD with predominant contamination obsessions and washing compulsions can learn to decrease (down-regulate) the blood oxygen level depended (BOLD) activity in the anterior insula using volitional control paired with rtfMRI in the presence of disgust-inducing stimuli.

The second aim of the study was to ascertain the feasibility and benefits of our method for a future larger study. Hence, in addition to evaluations related to clinical symptomatology measured by SCID-I, YBOCs, OCI-R, FEE, STAI and BDI-II, we included two behavioral assessments (Ecological Disgust Test-EDT and Picture Rating Test) designed to evaluate how self-regulation abilities affect individual responses towards disgust-inducing stimuli outside the scanner environment, in “real-life conditions”.

Furthermore, heart rate, respiration and eye-tracker measures were collected during the rtfMRI neurofeedback trainings in order to investigate the relationship of insula-control on autonomic functions.

Because head motion is frequently observed in patient populations during long fMRI sessions, we also aimed to investigate the effects of head motion on feedback to decide on the most feasible online motion correction algorithm to be used in our future study. Hence, we compared two widely used online motion correction algorithms in rtfMRI experiments in a parallel/technical study.

An overview of the experimental protocol can be seen in Table.1

1st Day	**2nd Day**	**3rd Day**	**4th 5th 6th 7th Days**	**8th Day**	**9th Day**	**10th Day**
*Screening Edinburgh Handedness Scale MWI *Pre-training clinical evaluation - SCID-I, - Y-BOCs, - FEE, - BDI-II, - STAI Trait.	Ecological Disgust Test (EDT) Pre-test.	Picture ratings and physiological measurements (SCR, HR) Pre-test	*rtfMRI-BCI trainings and transfer runs, *Inside the scanner-heart rate measurements, *Eye-tracker, * Diffusion Tensor Imaging (DTI) (on the 4th and 8th Days only) *STAI State.	Ecological Disgust Test (EDT) Post-test.	Picture ratings and physiological measurements (SCR, HR) Post-test	*Post-training clinical evaluation - Y-BOCs, - FEE.

Table. 1. Experimental protocol.

3. Self-regulation of anterior insula paired with rtfMRI in the presence of disgust-inducing stimuli.

RtfMRI trainings consisted of four training runs and one transfer run during which different disgust-inducing images from the International Affective Picture System (IAPS) (Lang, Bradley & Cuthbert, 2008) were presented to the OCD patients. Baseline blocks, (cued with a plus sign, "+") lasted for 30 seconds during which the patients were instructed to look directly at the screen, and to not suppress the feelings triggered by the images. For the down-regulation blocks (indicated by a down arrow "↓", for 27 seconds each), participants were instructed to find an effective cognitive strategy to decrease the feedback signal while viewing the disgust inducing images. No specific cognitive strategy was suggested to the participants. A feedback methodology based on monetary reward was used. Feedback was calculated and presented immediately following each down-regulation block (3 seconds). The amount of monetary feedback was calculated by using the following equation:

{meanBOLD[(ROI1 + ROI2)/2 - ROI3]Baseline - meanBOLD[(ROI1 + ROI2)/2 – ROI3]Down-regulation}*0.1

where the ROI1 and ROI2 correspond to the right and left anterior insula respectively and ROI3 is the reference ROI located in a non-active region close to the parietal cortex. Training runs with contingent feedback were interspersed with the "transfer runs" in which the patients were asked to down-regulate the ROIs without the aid of the feedback and by using the mental strategy learned during the neurofeedback training.

In the EDT, patients were confronted with real disgusting objects (e.g., chewed gum, used toilet paper) to investigate how learned insula self-regulation modulates the capability of the patients to bear the proximity of symptom-provoking objects. Disgusting objects in this test were selected individually for each patient according to his/her own self-report during the screening session. The object was placed in the first position on a wheeled table at a distance of five meters away from the patient. On the left side of this object, a clearly visible '+' sign or a '↓' sign was shown. In each trial, the selected object was slowly brought towards the patient at a constant pace either with the '+' sign or with the '↓' sign. Patients were instructed to focus on the object and say 'stop' when they felt that the object should not come any closer. On the post-test/down-regulation blocks, patients were instructed to use the cognitive strategies that they had learned during rtfMRI trainings to fight the disgust. The distances between the starting point and the point at the "stop" moment were measured for baseline and down-regulation blocks along the direction of movement of the experimenter for both pre-test and post-tests. In the picture-rating pre- and post-tests, patients rated disgust evoking pictures according to three different dimensions (valence, arousal and symptom provocation) outside the scanner through baseline and the down-regulation blocks. Patients were instructed to look at the pictures directly without suppressing the feelings that were triggered by the stimuli during the baseline blocks and to use the mental strategies that they had learned through the rtfMRI trainings during the down-regulation blocks. While looking at the pictures, physiological measures (skin conductance response and heart rate) were also recorded.

4. Effect of motion correction algorithms on feedback in real-time fMRI

Apart from the underlying neural activity, the noise from heart rate and respiration (Glover et. al., 2000; Noll & Schneider 1994), eye movements (Zhang et al., 2011) and head motion (Hajnal et al., 1994; Thacker et al., 1999; Friston et al., 1996) may also modulate the signal from fMRI. In rtfMRI experiments, the association between the mental strategy that successfully regulates a neural signal (behavior) and neurofeedback (consequence) can be affected negatively by this modulation (Schacter et al., 2011). Hence, to achieve efficient learning of brain self-control, a contingent feedback presented to the subjects by the rtfMRI system is crucial (Koush et al., 2012).

In contrast to conventional fMRI analysis with packages like SPM or FSL, in rtfMRI the time available for data pre-processing and statistical analysis is very limited. Therefore the processing pipeline includes only those steps that are considered to be essential and these are additionally optimized for data quality and speed. As subject motion would shift the brain and the region for feedback estimation, motion correction is an essential processing step.

In our second study we tested the consistency of feedback calculated from data preprocessed with two retrospective real time motion correction algorithms. The first algorithm is included in the image reconstruction of the MRI scanner's EPI sequence (3d k-space interpolation, Advanced Retrospective Technique, Siemens, Erlangen, Germany) and operates on the raw data in k-space. The second algorithm uses the data after Fourier transformation, i.e. the images, and is included in Turbo Brainvoyager (TBV, Brain Innovation, Maastricht, The Netherlands).

Under the assumption that both algorithms yield similar results, we expected a high correlation between the feedback values derived from the motion corrected data sets.

During the experiments TBV motion corrected data (TBV-MoCo, trilinear interpolation) had been used to calculate the feedback. Offline analysis of the Siemens-MoCo data was done analogously by TBV and our in-house plug in. TBV-MoCo is part of the TBV package and is executed on the rtfMRI computer whereas Siemens-MoCo is included in the image calculation on the MRI scanner. Both algorithms assume a rigid body model and estimate the optimal motion correction parameters iteratively. They stop after reaching a predefined threshold for the difference between the actual and the reference image or after reaching the maximal number of iterative steps. The resulting image is either calculated with a trilinear interpolation (TBV-MoCo) or a 3d k-space interpolation (Siemens-MoCo).

Pearson correlation coefficients for the motion correction parameters (three translation parameters, three rotation parameters) from TBV and Siemens as well as for the feedback values based on TBV-MoCo and Siemens-MoCo data were calculated for each run.

We additionally included an exponential moving average filter (EMA-filter) in the processing pipeline for TBV-MoCo and Siemens-MoCo data and calculated the reward parameter and the correlation with the unfiltered data.

As a last step, we tested the effect of two outlier removal strategies. We calculated the average signal and standard deviation for each voxel. Voxel values above two standard deviations from the average were marked as outliers within its data series. Our first outlier removal method rejected these outliers from the ROI averages. The second outlier removal method counted the number of voxels identified as outliers within one time point (volume) and included only time points in the calculation where the number of rejected voxels was below a predefined threshold. Method 1 is sensitive to noise within individual voxels. Method 2 is sensitive to global changes (e.g. head motion). Using this data we calculated again the feedback parameters and the correlations 'within' and 'between' the pipelines.

5. Results and Discussion

Recent evidence suggests that OCD with contamination obsessions and washing compulsions might be characterized by a disorder in disgust processing. The anterior insula hyperactivity may play a particularly important role in mediating such putative disruptions (Stein et al., 2006; Goetz et al., 2013; Starcevic et al., 2013). In the light of these findings, we designed a pilot study to explore the effects of rtfMRI based anterior insula down-regulation on several behavioral, physiological and clinical measures of OCD patients with contamination fears and washing compulsions. Also, we aimed to examine the feasibility of our study procedures, validity of the tools and our overall approach that is intended to be used in a larger future study. Yet, another purpose was to compare the effects of the two widely used online fMRI motion correction algorithms on feedback and decide on best correction algorithm to be used in the future study.

Our results show that anterior insula down-regulation is possible in OCD patients. In fact, all three patients could learn to decrease the BOLD signal in the anterior insula albeit to different degrees, in the presence of disgust inducing stimuli with rtfMRI. However, regarding the transfer runs, included to evaluate whether subjects could regulate anterior insula in absence of feedback, patients were less successful in self-regulation as compared with the regular training runs. Hence, in order to improve the behavioral results measured outside the scanner environment, improving the self-regulation ability in the absence of a real-time feedback with a design that includes more transfer runs would be crucial.

Yet, another step that can be taken to improve the success of the rtfMRI trainings would be about the feedback contingency. In rtfMRI experiments, the association between a mental strategy and feedback can be affected by the temporal delay of the feedback signal (Caria et al., 2010). In the great majority of rtfMRI studies, feedback is continuously presented with minimal delay, approximately around 2 seconds (Sulzer et al., 2013). Anterior insula displays strong functional connectivity with the anterior cingulate and in addition to its role in disgust processing, it has a role in feeling and motivation too (Craig, 2011). Hence, to prevent a possible activity increase in the insula due to reward processing itself, we averaged and presented the feedback information to the patients at the end of each down-regulation block in our design, in line with some previous rtfMRI studies (Bray et al., 2007; Posse et al., 2003; Shibata et al., 2011; Yoo and Jolesz, 2002). By doing this the feedback signal provided information about the monetary reward. Some studies however have suggested that intermittent feedback might be a better way to achieve a particular behavior –consequence association when mental imagery was used during self-regulation (Yoo & Jolesz, 2002; Johnson et al., 2012,). In this sense, providing feedback to patients about their ongoing brain activity at shorter intervals (e.g., every ten seconds) would be crucial for the future study. To avoid cognitive or visual distractions, which can be caused by the presence of an additional visual stimuli (e.g., a graphical thermometer next to the disgust inducing pictures in the screen), it would be beneficial to locate each picture inside a frame which can provide neurofeedback, for example by color changes. In this manner, it would be possible to separate the neurofeedback information from the reward, which will be presented at the end of each block.

In addition, the target regions selected for self-regulation and the self-regulation direction (either up or down) are crucial aspects in brain self-regulation experiments. The majority of previous rtfMRI studies used single ROI up-regulation paradigms in which participants had been trained to increase activity of one target region (for reviews please see Ruiz et al., 2013; Birbaumer et al., 2013; Sulzer et al., 2013). Up to now, fewer rtfMRI studies showed that subjects could learn to down-regulate the brain activity e.g., in amygdala (Brühl et al., 2014), subgenual anterior cingulate (Hamilton et al., 2011), auditory cortex (Haller, Birbaumer, and Veit 2010), anterior cingulate cortex (Li et al., 2012) and anterior insula (Caria et al., 2010; Veit et al., 2012; Li et al., 2012). Decreasing the BOLD activity might be harder as compared to increasing both in healthy and patient populations, although it might not be physiologically impossible as suggested by Logothetis and colleagues (2006). Our preliminary results are important in showing the possibility of down-regulation of an abnormally activated brain region in psychiatric populations. However, because OCD affects a distributed fronto-striatal circuit, a connectivity-based or a pattern classifier-based neurofeedback study design, instead of a single ROI design, might be an interesting possibility for future experimental designs.

Furthermore, to improve the self-regulation ability, a rtfMRI-EEG combined neurofeedback study design would be more beneficial. In that study design, EEG correlates of anterior insula self-regulation during the rtfMRI sessions with an MRI compatible EEG system can be recorded and later can be used use to train an EEG pattern classifier specific for each OCD patient. This data then would be used for the further EEG-based neurofedback trainings outside the scanner following the initial rtfMRI sessions. With that approach, self-regulation ability can be enhanced by increasing both the amount of the neurofeedback trainings and neurofeedback modalities.

Also, because of its ease of use and feasibility in general, extended neurofeedback training outside the scanner with portable functional near infrared spectroscopy (fNIRS) would be another option

As a pilot study with 3 patients, it is not possible to generalize conclusions regarding the behavioral effects of rtfMRI-BCI neurofeedback training and related symptomatological changes. In fact, behavioral and clinical effects of the rtfMRI-BCI neurofeedback training were not consistent in all patients. Two of the three patients of the study (patient 1 and patient 3) showed improvements in the EDT, picture rating test and the clinical assessments achieved by questionnaires. However, patient 2 did not display any improvement in these dimensions.

In two cases, patients improved their capability to bear the physical proximity of a real-world disgusting symptom-provoking object, using their learned cognitive strategies for down-regulation after the training. Showing the application of the learned brain self-regulation to the real-life conditions, these results are encouraging for the rtfMRI-BCI neurofeedback studies as most of the previous studies focused on immediate changes in the behaviors or symptoms happening inside the scanner environment (Caria et al., 2010; Sitaram et al 2012; Ruiz et al., 2013; Buyukturkoglu et al., 2013). In that manner, novel symptom-specific tests, like EDT, would be important to explore the transfer of learned self-regulation skills to “real-world” environments.

In parallel with the EDT results, the same two patients also showed improvements in the picture rating test in two dimensions i.e., valence and OCD symptom provocation. During the post-tests, patients rated the disgust evoking pictures with less negative valence and as less symptom provocative following down-regulation blocks.

Although patient 2 performed well during the rtfMRI-BCI neurofeedback training, she did not show an improvement in the behavioral or clinical measures. In fact, the patient's Y-BOCs scores were higher at the end of the experiments. Because the questionnaires used as clinical measures are self-administered and because we do not ask patients to use their mental strategies during the administration of the questionnaires, it is not possible to be certain whether the positive or negative changes in the scores could be attributed to the rtfMRI-BCI neurofeedback training or to other factors active during this period.

Non-consistent results were observed for HR measures collected inside the scanner. Two patients (patient 1 and patient 2), displayed decreased heart rates during the down-regulation conditions. However, patient 3 had higher heart rates while down-regulating through the runs. HR measures, recorded while the patients were looking to the disgust inducing pictures outside the scanner, did not reveal a significant difference between the baseline and the down-regulation conditions in the post-tests in all three patients.

Previous psycho-physiological investigations exploring responses towards disgust inducing stimuli are limited in number and provide conflicting results, including heart rate. Although some studies show elevated HR in the conditions when healthy subjects are presented with symptom provoking pictures (Lang, Bradley, & Cuthbert, 1997; Alaoui-Ismaili et al., 1997; Schienle et al., 2001; Vrana, 1994), others point to a deceleration in the HR as an indicator of parasympathetic activity (Gross, 1998; Gross & Levenson, 1993; Johnsen, Thayer, & Hugdahl, 1995; Levenson, 1992). Studies that have measured OCD patients' physiological responses towards disgust inducing stimuli reported contradictory results as well. While some experimenters found elevated autonomic nervous system activity and HR (Benkelfat et al., 1991; Insel, Zahn, & Murphy, 1985; Rabavilas, Boulougouris, & Stefanis, 1977; Stein et al., 2006), other studies reported HR decelerations which is interpreted as a sign of orientation and not avoidance or stimulus rejection (Hoehn-Saric, McLeod, & Hipsley, 1995; Hollander et al., 1991; McCarthy, Ray, & Foa, 1995; Zahn, Leonard, Swedo, & Rapoport, 1996). One of the reasons for these conflicting findings might be the type of the stimuli used in the experiments. While the disgust emotion elicited in relation to contamination and pollution (e.g., pictures of dirty toilets, cockroaches, maggots on food, foul smells, facial expressions of expelling food), is characterized by HR acceleration, disgust elicited in relation to mutilation, injury and blood (e.g., injections, mutilation scenes, bloody injuries), seems to be characterized by a pattern of HR deceleration (Olantuji et al., 2013). In our set of stimuli we included both contamination and mutilation types of images. Therefore, and depending on the heterogeneity of the OCD patients, using both kinds of pictures together in the same measurement might cause a neutralizing effect in HR measures. The differences on anxiety levels in our small group of patients might have also contributed to this inconsistency in HR results. Patient 3, who showed elevated HR during the down-regulation conditions in the scanner, showed also the highest anxiety level (both in trait and state-anxiety measures). Patients' elevated HR during down-regulation conditions might be also attributed to a high performance anxiety and reward expectancies.

Disgust is consistently reported to be associated with increased electrodermal activity (Olantuji et al., 2013). However, we did not observe a significant difference between disgust provoking and neutral pictures and skin conductance response levels. There were no significant differences in levels between baseline and down-regulation blocks while patients were viewing disgust inducing pictures either. Because we measured the mean skin conductance levels throughout baseline and the down-regulation blocks, these results might be due to the presentation of mixed type of disgust inducing pictures.

Because avoidance is a frequently observed response of the OCD patients (Starcevic et al., 2013), we wanted to be sure that the participants in the current study were consistently observing the presented pictures through the measurements. Inside the scanner, and through the rtfMRI-BCI trainings, we used an eye-tracker system for this purpose. The eye tracker system measured pupil location coordinates and size changes during the presentation of each picture. The preliminary analysis of eye tracker data confirmed that every patient of the study looked directly at the disgust inducing images throughout the runs. Apart from the sympathetic-parasympathetic effects on the pupil size and eye-blinks, these measurements are essential for future studies to ensure that patients observe the stimuli presented to them despite their highly disturbing nature.

The basic idea of neurofeedback with rtfMRI is to provide the subject with correct information about signal changes in the brain. In this sense, in addition to behavioral, clinical and physiological measures, we also explored the effects of two online motion correction algorithms on the feedback that is presented to the patients. As our calculation included averaging over a long period of time and extended regions of interest, the temporal and spatial noise is smoothed out and we expected a good linear correlation of the results from the two pre-processing pipelines as long as the motion correction algorithms work fine.

We found however in more than 30 percent of the runs incongruent feedback value, i.e. the correlation between feedback calculated from TBV-MoCo data and feedback calculated from Siemens-MoCo data was low.

In some runs, while one processing pipeline provided a positive feedback value, the other gave a negative value of the same size. This still happens when the absolute motion is small and the correlation of the motion correction parameters is high. So even small differences between the two algorithms can give rise to a relevant difference in the feedback.

To improve the correlation of the feedback values between the different MoCo algorithms, we tested an EMA-filter and two simple outlier removal strategies. The EMA-filter had little effect on the data and did not improve the correlation between the pipelines. The first outlier removal strategy (rejecting individual voxel data) worsened the results, but the second strategy (rejecting whole ROI data for individual time points) seems promising. Still we need to identify optimal parameters and we have to test the effect on different feedback estimations, i.e. continuous and/or intermittent feedback.

Right now, it is not obvious which pipeline provides better feedback, but wrong feedback information will increase the level of difficulty for the subject to identify an effective training strategy and can therefore prolong the training. Further studies should include simulations to decide on optimal data preprocessing.

We can only conclude from a low correlation between the two preprocessing pipelines that the feedback quality will be poor in at least one of them. From a high correlation between the pipelines we learn that the feedback parameter calculation is robust according to the processing pipelines, but this does not implicate a correct feedback.

6. Conclusion

In this pilot study we investigated the application of rtfMRI neurofeedback for anterior insula regulation in OCD patients. We also explored the feasibility of several behavioral and physiological pre- and post-training tests and clinical assessments that would be used in a future long-term study. Our results indicate that with sufficient training, OCD patients can learn to down-regulate the BOLD activity in their anterior insula in the presence of disgust inducing stimuli. The two tests that were designed to examine the effect of this self-control in real-world conditions outside the scanner (picture rating tests and the EDT) have important implications for future studies.

In a parallel/technical study, we compared two fMRI online motion correction algorithms in the manner of their effects on feedback. The results suggest a relevant dependence of the feedback from the motion correction algorithm. Restricting subject head movement remains a strong prerequisite for rtfMRI experiments. But as even small movements led to differences in the feedback, the robustness of the feedback parameter must be tested in future studies with respect to motion.

7. References

1. Alaoui-Ismaili, O., Robin, O., Rada, H., Dittmar, A., & Vernet-Maury, E. (1997). Basic emotions evoked by odorants: comparison between autonomic responses and self-evaluation. Physiology & Behaviour, 62, 713–720.

2. Aouizerate B, Guehl D, Cuny E, Rougier A, Bioulac B, et al. (2004). Pathophysiology of obsessive-compulsive disorder: a necessary link between phenomenology, neuropsychology, imagery and physiology. ProgNeurobiol72:195–221.
   [1] APA – American Psychiatric Association. (2000). Diagnostic and Statistical Manual of Mental Disorders – DSM-IV-TR (4th edition, Text Revision). Washington, D.C.: American Psychiatric Association.´

3. Benkelfat, C., Mefford, I. N., Masters, C. F., Nordahl, T. E., King, A. C., Cohen, R. M., et al. (1991). Plasma catecholamines and their metabolites in obsessive-compulsive disorder. PsychiatryResearch,37(3),321–331.

4. Bray, S., Shimojo, S., O'Doherty, J.P., 2007. Direct instrumental conditioning of neural activitusing functional magnetic resonance imaging-derived reward feedback. J. Neurosci. 27 (28), 7498–7507.

5. Birbaumer N, Ruiz S, Sitaram R. (2013). Learned regulation of brain metabolism. Trends Cogn Sci. Jun;17(6):295-302.

6. Buyukturkoglu, K., Rana, M., Ruiz, S., Hackley, S. A. , Soekadar, S. R., Birbaumer, N., Sitaram, R. (2013). Volitional Regulation of the Supplementary Motor Area with fMRI-BCI neurofeedback in Parkinson’s disease: A Pilot Study. Conference Proceeding. Neural Engineering (NER), 6th International IEEE/EMBS Conference on 6-8Nov2013.SanDiego,CA.Page(s):677–681.

7. Caria, A., Sitaram, R., Birbaumer, N., 2012. Real-time fMRI: a tool for local brain regulation. Neuroscientist18(5).487–501.

8. Caria, A., Sitaram, R., Veit, R., Begliomini, C., Birbaumer, N., 2010. Volitional control of anterior insula activity modulates the response to aversive stimuli. A real-time functional magnetic resonance imagingstudy.Biol.Psychiatry68(5),425–432.

9. Caria, A., Veit, R., Sitaram, R., Lotze, M., Weiskopf, N., Grodd, W., Birbaumer, N., 2007. Regulation of anterior insular cortex activity using real-time fMRI. NeuroImage 35 (3), 1238–1246.

10. Cisler, J. M., Olatunji, B. O., & Lohr, J. M. (2009). Disgust, fear, and the anxiety disorders: A critical review. JournalofAnxietyDisorders,29(1)34–46.

11. Cox, R.W., Jesmanowicz, A., 1999. Real-time 3D image registration for functional MRI. Magn. Reson. Med. 42, 1014 – 1018.

12. Craig, B., (2011). How do you feel - now? The anterior insula and human awareness. Nat. Rev. Neurosci. 10, 59–70

13. Friston, K.J., Williams, S., Howard, R., Frackowiak, R.S.J., Turner, R., 1996. Movement-related effects in fMRI time series. Magn. Reson. Med. 35, 346 – 355.

14. Glover, G.H., Li, T.Q., Ress, D. (2000). Image-based method for retrospective correction of physiological motion effects in fMRI: RETROICOR. Magn. Reson. Med. 44, 162–167.

15. Gross, J. J. (1998). Antecedent- and response-focused emotion regulation: Divergent consequences for experience, expression, and physiology. Journal of Personality and Social Psychology, 74(1), 224–237

16. Hajnal, J.V., Myers, R., Oatridge, A., Schwieso, J.E., Young, I.R., Bydder, G.M., 1994. Artifacts due to stimulus correlated motion in functional imaging of the brain. Magn. Reson. Med. 31, 283 – 291.

17. Haller, S., Birbaumer, N., Veit, R., 2010. Real-time fMRI feedback training may improve chronic tinnitus. Eur. Radiol. 20 (3), 696–703.

18. Hamilton, J.P., Glover, G.H., Hsu, J.J., Johnson, R.F., Gotlib, I.H., 2011. Modulation of subgenual anterior cingulate cortex activity with real-time neurofeedback. Human Brain Mapping. 32 (1), 22–31.

19. Hoehn-Saric, R., McLeod, D. R., & Hipsley, P. (1995). Is hyperarousal essential to obsessive compulsive disorder? Diminished physiologic flexibility, but not hyperarousal, characterizes patients with obsessive-compulsive disorder. Archives of General Psychiatry, 52(8), 688–693.

20. Hollander, E., DeCaria, C., Nitescu, A., Cooper, T., Stover, B., Gully, R., et al. (1991). Noradrenergic function in obsessive-compulsive disorder: behavioral and neuroendocrine responses to clonidine and comparison to healthy controls. Psychiatry Research, 37(2), 161–177.

21. Insel, T. R., Zahn, T., & Murphy, D. L. (1985). Obsessive–compulsive disorder: an anxiety disorder. In: A. T. Tuma, & J. Maser (Eds.), Anxiety and the anxiety disorders (pp. 577–589). Hillsdale, NJ: Lawrence Erlbaum & Associates.

22. Johnsen, B. H., Thayer, J. F., & Hugdahl, K. (1995). Affective judgment of the Ekman faces: A dimensional approach. Journal of Psychophysiology, 9(3), 193–202.

23. Johnson, K.A., Hartwell, K., LeMatty, T., Borckardt, J., Morgan, P.S., Govindarajan, K., Brady, K., George, M.S., 2012. Intermittent "real-time" fMRI feedback is superior to continuous presentation for a motor imagery task: a pilot study. J. Neuroimaging 22 (1), 58–66.

24. Koush Y, Zvyagintsev M, Dyck M, Mathiak KA, Mathiak K. (2012). Signal quality and Bayesian signal processing in neurofeedback based on real-time fMRI. Neuroimage. Jan 2;59(1):478-89.

25. Lang, P. J., Bradley, M. M., & Cuthbert, B. N. (1997). Motivated attention: affect, activation, and action. In: P. J. Lang, R. F. Simons, & M. Balaban (Eds.), Attention and orienting: sensory and motivational processes (pp. 97–135). Hillsdale, NJ: Lawrence Erlbaum Associates.

26. Lang, P. J., Bradley, M. M., & Cuthbert, B. N. (2008). International affective picture system (IAPS): affective ratings of pictures and instruction manual. Technical report A-6. Gainesville, FL: Center for Research in Psychophysiology, University of Florida.

27. Levenson, R. W. (1992). Autonomic nervous system differences among emotions. Psychological Science, 3(1), 23–27.

28. Li, X., Hartwell, K.J., Borckardt, J., Prisciandaro, J.J., Saladin, M.E., Morgan, P.S., Johnson, K.A., LeMatty, T., Brady, K.T., George, M.S., 2012. Volitional reduction of anterior cingulate cortex activity produces decreased cue craving in smoking cessation: a preliminary real-time fMRI study. Addict. Biol.

29. Linden, D. E., Habes, I., Johnston, S. J., Linden, S., Tatineni, R., Subramanian, L., Sorger, B., Healy, D., & Goebel, R. (2012). Real-time self-regulation of emotion networks in patients with depression. PLoS ONE, 7, e38115.

30. Mataix-Cols, D., Wooderson, S., Lawrence, N., Brammer, MJ., Speckens, A., Phillips, ML. (2004). Distinct neural correlates of washing, checking, and hoarding symptom dimensions in obsessive-compulsive disorder. Arch Gen Psychiatry. 61(6):564-76.

31. McCarthy, P. R., Ray, W. J., & Foa, E. B. (1995). Cognitive influences on electrocortical and heart rate activity in obsessive-compulsive disorder. International Journal of Psychophysiology, 19(3), 215–222.

32. Menzies L, Chamberlain SR, Laird AR, Thelen SM, Sahakian BJ, Bullmore ET. Integrating evidence from neuroimaging and neuropsychological studies of obsessive-compulsive disorder: the orbitofronto-striatal model revisited. Neurosci Biobehav Rev. 2008;32(3):525-549.

33. Moretz, M.W., McKay, D. (2008). Disgust sensitivity as a predictor of obsessive-compulsive contamination symptoms and associated cognitions. J Anxiety Disord. 22(4):707-15.

34. Noll DC, Schneider W. Theory, simulation and compensation of physiological motion artifacts in functional MRI. In: Proceedings of IEEE International Conference on Image Processing, Austin, Texas, 1994. p40.

35. Olatunji, B. O., Cisler, J. M., Deacon, B. J., Connolly, K., & Lohr, J. M. (2007). The disgust propensity and sensitivity scale-revised: Psychometric properties and specificity in relation to anxiety disorder symptoms. Journal of Anxiety Disorders, 21, 918–930.

36. Olatunji, B. O., Sawchuk, C. N. (2013). Disgust domains in the prediction of contamination fear. Behaviour Research and Therapy, 42, 93–104.

37. Olatunji, B. O., Sawchuk, C. N., Lohr, J. M., & de Jong, P. J. (2004). Disgust domains in the prediction of contamination fear. Behaviour Research and Therapy, 42, 93–104.

38. Phillips, ML., Marks, IM., Senior, C., Lythgoe, D., O'Dwyer, AM., Meehan, O., Williams, SC., Brammer, MJ., Bullmore, ET., McGuire, PK. (2000). A differential neural response in obsessive-compulsive disorder patients with washing compared with checking symptoms to disgust. Psychol Med. 30(5):1037-50.

39. Posse, S., Fitzgerald, D., Gao, K., Habel, U., Rosenberg, D., Moore, G.J., Schneider, F., 2003. Real-time fMRI of temporolimbic regions detects amygdala activation during single-trial self-induced sadness. NeuroImage 18 (3), 760–768.

40. Rabavilas, A. D., Boulougouris, J. C., & Stefanis, C. (1977). Synchrony and concordance on subjective and psychophysiological measures after beta-blockade and flooding in obsessive–compulsive patients. In: J. C. Boulougouris, & A. D. Rabavilas (Eds.), The treatment of phobic and obsessive-compulsive patients (pp. 115–125). Oxford: Pergamon.

41. Rachman, S. (2004). Fear of contamination. Behaviour Research and Therapy, 42(11), 1227–1255.

42. Ruiz, S., Buyukturkoglu, K., Rana, M., Birbaumer, N., Sitaram, R. (2013). Real-time fMRI brain computer interfaces: Self-regulation of single brain regions to networks . Biol Psychol. 2014 Jan;95:4-20

43. Ruiz, S., Sitaram, R., Lee, S., Soekadar, S., Caria, A., Veit, R., Kircher, T., Birbaumer, N., Sitaram, R. (2011b). Acquired self-control of insula cortex modulates emotion recognition and brain network connectivity in schizophrenia. Human Brain Mapping.

44. Ruscio, AM., Stein, DJ., Chiu, WT., Kessler, RC. (2010) The epidemiology of obsessive-compulsive disorder in the National Comorbidity Survey Replication. Mol Psychiatry. 15 (1):53-63. Epub 2008 Aug 26.

45. Schienle, A., Schäfer, A., Stark, R., Walter, B., Kirsch, P., & Vaitl, D. (2003). Disgust processing in phobia of blood–injection–injury: an fMRI study. Journal of Psychophysiology, 17, 87–93.

46. Schienle, A., Stark, R., & Vaitl, D. (2001). Evaluative conditioning: A possible explanation for the acquisition of disgust responses? Learning and Motivation, 32(1), 65–83.

47. Shapira, N. A., Liu, Y., He, A. G., Bradley, M. M., Lessig, M. C., James, G. A., Goodman, W. K. (2003). Brain activation by disgust-inducing pictures in obsessive-compulsive disorder. Biological Psychiatry, 54(7), 751–756.

48. Sitaram, R., Caria, A., Veit, R., Gaber, T. (2008a). Volitional control of insula using an fMRI Brain-Computer Interface in criminal psychopaths enhances functional connectivity of the emotional network. 38th annual meeting of the Society for Neuroscience, Washington

49. Sitaram, R., Lee, S., Ruiz, S., Rana, M., Veit, R., Birbaumer, N. (2010). Real-time support vector classification and feedback of multiple emotional brain states. Neuroimage. May 15;56(2):753-65.

50. Sitaram, R., Veit, R., Stevens, B., Caria, A., Gerloff, C., Birbaumer, N., Hummel, F. (2012). Acquired control of ventral premotor cortex activity by feedback training: an exploratory real-time FMRI and TMS study. Neurorehabil Neural Repair. Mar-Apr;26(3):256-65.

51. Stein, D. J., Arya, M., Pietrini, P., Rapoport, J. L., & Swedo, S. E. (2006). Neurocircuitry of disgust and anxiety in obsessive-compulsive disorder: a positron emission tomography study. Metabolic Brain Disease, 21(2–3), 267–277.

52. Sulzer J, Haller S, Scharnowski F, Weiskopf N, Birbaumer N, Blefari ML, Bruehl AB, Cohen LG, DeCharms RC, Gassert R, Goebel R, Herwig U, LaConte S, Linden D, Luft A, Seifritz E, Sitaram R. (2013). Real-time fMRI neurofeedback: progress and challenges. Neuroimage. Aug 1;76: 386-99.

53. Thacker, N.A., Burton, E., Lacey, A.J., Jackson, A., 1999. The effects of motion on parametric fMRI analysis techniques. Physiol. Meas. 20, 251 – 263.

54. Veit, R., Singh, V., Sitaram, R., Caria, A., Rauss, K., Birbaumer, N., 2012. Using real-time fMRI to learn voluntary regulation of the anterior insula in the presence of threat-related stimuli. Soc. Cogn. Affect. Neurosci. 7 (6), 623–634.

55. Vrana, S. R. (1994). Startle reflex response during sensory modality specific disgust, anger, and neutral imagery. Journal of Psychophysiology, 8(3), 211–218.

56. Yoo, S.S., Jolesz, F.A., (2002). Functional MRI for neurofeedback: feasibility study on a hand motor task. Neuroreport 13 (11), 1377.

57. Zahn, T. P., Leonard, H. L., Swedo, S. E., & Rapoport, J. L. (1996). Autonomic activity in children and adolescents with obsessive-compulsive disorder. Psychiatry Research, 60(1), 67–76.

8. List of publications and statement of contributions

1. Buyukturkoglu K, Rana M, Ruiz S, Hackley S. A, Soekadar S. R, Birbaumer N, Sitaram R. (2013). Volitional Regulation of the Supplementary Motor Area with fMRI-BCI neurofeedback in Parkinson's disease: A Pilot Study. Conference Proceeding. Neural Engineering (NER), 6th International IEEE/EMBS Conference on 6-8 Nov2013. San Diego, CA. Page(s): 677-681 ISSN: 1948-3546 INSPEC Accession Number: 14001780 10.1109/NER.2013.6696025. (Published paper).

I have conducted the experiments with Mohit Rana. I did the analysis, statistics and wrote the manuscript. Dr. Sitaram and Dr. Birbaumer were my supervisors and they reviewed the manuscript. Dr. Ruiz, Dr. Hackley and Dr. Soekadar reviewed the manuscript. This work was mainly supervised by Dr. Ranganatha Sitaram during all the process of work.

2. Ruiz S, Buyukturkoglu K, Rana M, Birbaumer N, Sitaram R. (2014). Real-time fMRI brain computer interfaces: Self-regulation of single brain regions to networks Biol Psychol.2014 Jan; 95:4-20. Doi10.1016/j.biopsycho.2013.04.010. Epub 2013 May. (Published paper).

I have prepared the Real-time fMRI brain computer interfaces: Self-regulation of single brain regions part of this publication. Mohit Rana has prepared the networks part. Dr. Sitaram and Dr. Birbaumer reviewed the manuscript. This work was mainly done by Dr. Sergio Ruiz during all the process of work.

3. Buyukturkoglu K, Roettgers H, Sommer J, Rana M, Dietzsch L, Arikan E, Kircher T, Birbaumer N, Sitaram R. Ruiz S.(2014). Self-regulation of anterior insula with rea-time fMRI and behavioral effects in obsessive compulsive disorder. Frontiers in Neuroscience. Hosting Specialty: Frontiers in Behavioral Neuroscience, Research Topic Title: Learned brain self-regulation for emotional processing and attentional modulation: from theory to clinical applications. (Under revision).

I have conducted the experiments with Leonie Dietzsch, Dr. Roettgers and Dr. Sommer. Mohit Rana wrote the presentation codes. I did the analysis, statistics and I wrote the manuscript. Dr. Sitaram, Dr. Kircher, Dr. Birbaumer reviewed the manuscript. This work was mainly supervised by Dr. Ruiz, Dr. Sitaram and Dr. Birbaumer during all the process of work.

4. Buyukturkoglu K, Rana M, Dietzsch L, Arikan B.E, Rana M, Ruiz S, Kircher T, Sitaram R, Roettgers H. Sommer J, (2014). (Under revision). Effect of Motion correction Algorithms on Feedback in Real-time fMRI. Frontiers in Neuroscience. Hosting Specialty: Frontiers in Behavioral Neuroscience, Research Topic Title: Learned brain self- regulation for emotional processing and attentional modulation: from theory to clinical applications.(Under revision).

I have conducted the experiments with Leonie Dietzsch and Dr. Sommer. Dr. Sommer did the analysis. Dr. Sommer and I wrote the manuscript. Dr. Kircher, Dr. Sitaram, Dr. Birbaumer and Dr. Ruiz reviewed the manuscript. This work was mainly supervised by Dr. Jens Sommer during all the process of work.

Chapter 2. Original articles and manuscripts

2.1. Self-regulation of anterior insula with real-time fMRI and behavioral effects in obsessive compulsive disorder: A Pilot study (Submitted Manuscript)

Buyukturkoglu K, Roettgers H, Sommer J, Rana M, Dietzsch L, Arikan E, Kircher T, Birbaumer N, Sitaram R. Ruiz S. (2014). (under revision). Frontiers in Neuroscience. Hosting Specialty: Frontiers in Behavioral Neuroscience, Research Topic Title: Learned brain self-regulation for emotional processing and attention modulation: from theory to clinical applications.

Introduction

Obsessive-compulsive disorder (OCD) is a condition that affects about xx percent of the population. It can have disabling effects throughout the patient's lifespan. To be diagnosed with OCD, a person must have obsessions and/or compulsions (DSM-IV-TR, 2000). Among the most common obsessions are contamination fears (usually followed by washing compulsions), which are intense and intrusive feelings of being polluted or infected by contact with the dirty, infectious or soiled objects (Rachman, 2004; Broderick, Grisham & Weidmann, 2013).

The exploration of the neural basis of OCD with fMRI has revealed an abnormal activation of several brain areas including the prefrontal cortex, orbitofrontal cortex, cingulate gyrus, thalamus, putamen and globus pallidus (Millet et al., 2013). Hence, current models of the disease hypothesize a dysfunction in the cortico-subcortical circuitry (Greybiel & Rauch, 2000; Aouizerate et al., 2004; Menzies et al., 2008). More recent efforts have tried to elucidate its neural basis in concordance with the heterogenic presentation of the disorder.

In this sense, several studies have shown a link between contamination fears, disgust over-reactivity and insula activation. Although, activation in the insula is associated with many interoceptive/subjective feelings (e.g., pain, temperature, or itch stimuli) the anterior part of this paralimbic structure is involved in disgust processing as a part of the gustatory cortex, containing neurons that respond to pleasant and unpleasant taste (Craig, 2011; Wright et al., 2004; Rolls, 1994).

Several sources of evidence support the aforementioned link between contamination fears, disgust over-reactivity and insula activation. First, disgust, which might be triggered by actual or perceived threat of contamination with the objects considered to be unclean, infectious or corrupted, is strongly associated with the fear of contamination and subsequent washing compulsions (Broderick, Grisham & Weidmann, 2013; Olatunji et al., 2004; Stein et al., 2006). Furthermore, heightened disgust feelings towards disgust-inducing stimuli and greater behavioral avoidance from disgusting objects, situations and places are commonly observed in OCD patients, especially those with contamination fears and washing compulsions (Starcevic et al., 2013, Olantuji et al., 2007, Tsao & McKay, 2004; Cisler et. al, 2010; Muris et. al, 2008; Schienle et. al, 2003; Schienle et al., 2005; Phillips et al., 2000; Sieg and Scholz, 2001: Moretz et al., 2008; Goetz et al., 2013). On the other hand, findings from functional neuroimaging studies (including functional magnetic resonance imaging-fMRI and positron emission tomography-PET) have indicated that, when subjects are presented with disgust inducing stimuli, the insula is activated in persons with OCD, especially in the group of patients with contamination fears (Phillips, 2000; Shapira, 2003; Stein et al., 2006). In summary there is strong evidence that an over-activation in the anterior part of the insular cortex, and disgust over-reactivity contribute to avoidance and ritualistic behaviors by increasing the aversiveness of exposure to certain stimuli, and strengthening beliefs about contamination (Berle & Phillips, 2006).

These results suggest that a reduction of insula activity should enable a reduction in contamination anxiety in the subgroup of OCD patients with predominantly contamination fears and washing compulsions.

Brain-Computer Interfaces (BCIs) utilize neurophysiological brain signals to activate or deactivate external devices or computers (Birbaumer & Cohen, 2007). With the introduction of real-time functional magnetic resonance imaging (rtfMRI), voluntary control over specific brain areas was achieved with rtfMRI-BCI neurofeedback both in healthy participants (e.g., Caria et al., 2007, 2010; Veit et al., 2012, Lawrence et al., 2014, Sitaram et al., 2010) and people suffering from neuropsychiatric diseases, such as schizophrenia and depression (e.g., Sitaram, 2008a; Sitaram et al., 2012; Ruiz et al., 2013; Linden et al., 2012). (For detailed reviews see Ruiz et al., 2013; Birbaumer et al., 2013; Sulzer et al., 2013).

In a recent study, Scheinost and colleagues (2013) explored the effect of rtfMRI-BCI neurofeedback training on healthy individuals without a clinical diagnosis of anxiety disorder, but who suffered from contamination anxiety while presented with disgust inducing stimuli. Participants who successfully learned to control the activity of orbitofrontal cortex displayed changes in resting-state connectivity across different brain areas and an enhanced control over contamination anxiety many days after the completion the training. These results encourage the application of rtfMRI neurofeedback in OCD patients.

Therefore we designed a pilot rtfMRI case series-study in OCD patients, with two major aims. Our first aim was to investigate whether patients suffering from OCD with predominantly contamination obsessions and washing compulsions can learn to volitionally decrease (down-regulate) the blood oxygen level depended (BOLD) activity in the anterior insula. Our second aim was to evaluate the effect of down-regulation training on clinical, behavioral and physiological changes pertaining to OCD symptoms. The larger goal of this study is to ascertain the feasibility and benefits our method for a future larger study. Hence, in addition to evaluations related to clinical symptomatology, we include three assessments designed to evaluate how self-regulation affects individual responses towards disgust inducing stimuli outside the scanner environment: 1) a test conducted in real-life conditions, hereafter termed the ecological disgust test (EDT). In the EDT, patients were confronted with real disgusting objects (e.g., chewed gums, used toilet papers) to investigate how learned insula self-regulation modulates the capability of the patients to bear the proximity of a symptom-provoking object. 2) A disgust inducing picture-rating test. In the picture-rating test, patients rated disgust evoking pictures in different dimensions (valence, arousal and symptom provocation) outside the scanner by using the mental strategy to fight the disgust learned during rtfMRI trainings. While looking at the pictures, physiological measures, namely skin conductance response and heart rate variability were recorded. 3.) During the rtfMRI-BCI neurofeedback trainings, variability of heart rate and pupil size were measured in order to investigate the relationship of insula control on autonomic functions.

Methods

Participants:

In this pilot study, 3 adult patients (2 females) with DSM IV diagnosed OCD from the Department of Psychiatry and Psychotherapy, University of Marburg took part. They were selected among a larger group of OCD patients, because they suffered from pronounced contamination obsessions and washing compulsions, as confirmed by a standardized clinical interview. All participants gave their written informed consent before participation. This study was approved by the local ethics committee of the Faculty of Medicine, University of Marburg.

Experimental protocol:

To measure the effects of rtfMRI-BCI neurofeedback training on OCD patients, we applied several pre- and post-training tests. Between the pre- and post-test, patients underwent several sessions of rtfMRI neurofeedback training. During the neurofeedback sessions, patients were trained to down-regulate the BOLD signal extracted from the left and right anterior insula cortex. Pre and post-tests were composed of the same measurements, but in the post-tests patients used the cognitive strategies learned inside the scanner during the training sessions to down-regulate the anterior insula. The experimental protocol included 10 days of testing and training for each participant, see table 1 and below.

Screening:

On the first day of the study, a trained psychologist administered the scales and questionnaires and obtained basic demographic information (gender, age, educational background), duration of the disease, previous psychotropic medications, and years using psychopharmacological medication. A vocabulary test as a measure of verbal intelligence (Mehrfachwahl-Wortschatz-Intelligenztest MWI; Lehrl, 1999), and the Edinburgh Handedness Inventory (Oldfield, 1971) were also applied.

Pre-training clinical evaluation:

The pre-training clinical evaluation included the following psychometric questionnaires and scales:

The German version of the Yale-Brown Obsessive Compulsive Scale (Y-BOCs) interview was used in order to assess the severity of OCD symptoms (Hand et al., 1991). A score higher than 10 for compulsive acts or obsessions indicates clinically relevant OCD pathology. If there are compulsions and obsessions score > 16 is clinically relevant (Hand et al.1991).

The German version of the Beck Depression Inventory (BDI-II, Hautzinger et al., 2009) was used to measure depression. A score > 18 indicates clinically relevant depression.

The German version of the state-trait-anxiety inventory (STAI) was used for measuring trait and state anxiety (Laux et al., 1981). Participants had to show on a 4-point-Likert scale the degree of fear elicited by 40 stimuli (20 for trait anxiety, 20 for state anxiety). For the trait versions the scores can be translated into T-scores between different comparison groups considering gender, age and psychiatric disorder, such as, depression. For the state version, there are no standard specifications. The healthy validation sample showed a mean-score of 36.84 (SD = 9.82 female) and 38.09 (SD =20.30, male) (Laux et al., 1981).

To quantify the degree of sensitivity to disgust stimuli Fragebogen zur Erfassung der Ekelempfindlichkeit (FEE) was used (Schienle et al., 2002). This questionnaire measures on a 5-point Likert scale with 37 items the participant's disgust sensitivity classified under 5 sub-scales (death, foulness, hygiene, oral defense and secretion). An overall mean score > 2.63 indicates elevated level of disgust sensitivity.

1st Day	2nd Day	3rd Day	4th 5th 6th 7th Day	8th Day	9th Day	10th Day
*Screening -Edinburgh Handedness Scale -MWI *Pre-training clinical evaluation - SCID-I - Y-BOCs - FEE - BDI-II - STAI Trait	Ecological Disgust Test (EDT) Pre-test	Picture ratings and physiological measurements (SCR, HRV) Pre-test	*rtfMRI-BCI trainings and transfer runs *Inside the scanner-heart rate measurements *Eye-tracker * Diffusion Tensor Imaging (DTI) (on the 4th and 8th Days only) *STAI State	Ecological Disgust Test (EDT) Post-test.	Picture ratings and physiological measurements (SCR, HRV) Post-test	*Post-training clinical evaluation - Y-BOCs, - FEE

Table 1. *Experimental Protocol.*

Real time fMRI-BCI neurofeedback training:

On the first day of rtfMRI-BCI neurofeedback training, following a functional localizer run and a structural scan, the regions of interest (ROI1: left anterior insula and ROI2: right anterior insula) were selected. We used both structural and functional information for ROI selection, as the combined method improves the accuracy of ROI selection and is considered to be clinically more useful (Lawrence et al., 2014). The primary motor area was selected as a reference ROI, namely ROI3, to cancel out the effect of movement related activation and global, unspecific activations, and to nullify the effect of an imprecise activation on feedback.

Each rtfMRI-BCI neurofeedback session consisted of 4 training runs. Each training run consisted of 6 alternating blocks of baseline, down-regulation and neurofeedback/reward blocks. During baseline and down-regulation blocks disgust inducing images (e.g., pictures of body waste, rotten food, blood injury, rats, cockroaches, dead animal corpses and vomit, selected from the International Affective Picture System (IAPS), (Lang, Bradley & Cuthbert, 2008) were projected on a screen at the back of the MRI scanner and presented to the patients via a mirror mounted on the head coil of the MRI.

Baseline blocks were indicated by the discriminating stimulus, plus sign ('+'), on the right side of each disgust inducing image. Every block lasted for 30 seconds during which the participants were instructed to look directly at the screen, view the images and not suppress the feelings triggered by these images. For the down-regulation blocks (indicated by the discriminating stimulus, down arrow (↓), on the right side of the picture, 27 seconds each), participants were instructed to find an effective cognitive strategy to decrease the feedback signal while viewing the disgust inducing images. No specific cognitive strategy was suggested to the participants. Every disgust inducing image was used for both baseline and down-regulation blocks separately at least once through the runs.

A feedback methodology based on monetary reward was used. Feedback was calculated and presented immediately following each down-regulation block (3 seconds). The amount of monetary feedback was calculated by using the following equation:

$$\{meanBOLD[(ROI1 + ROI2)/2 - ROI3]_{Baseline} - meanBOLD[(ROI1 + ROI2)/2 - ROI3]_{Down\text{-}regulation}\}*0.1$$

Figure 1. displays the flow the rtfMRI training runs.

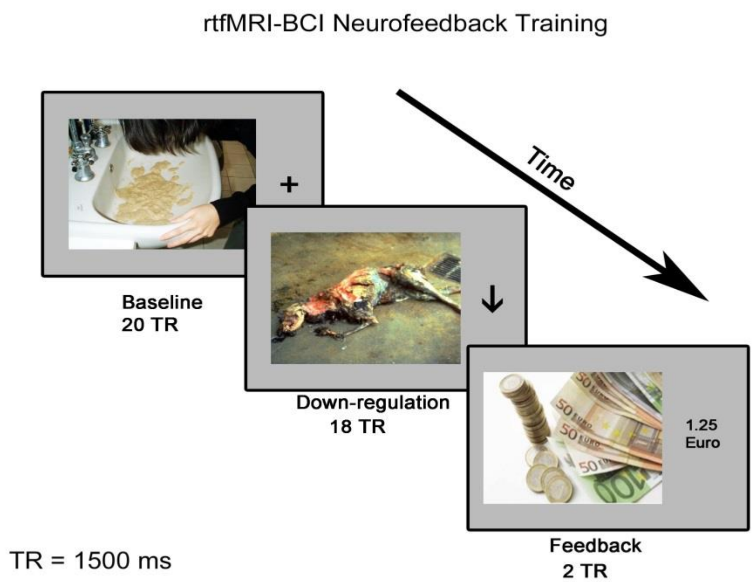

Figure 1. *Flow of the rtfMRI-BCI neurofeedback training run. Each run consisted of 6 baseline (duration: 30 seconds each) and 6 down-regulation blocks (duration: 27 seconds each). Immediately following each block of down-regulation, a monetary feedback was presented for 3 seconds. The same design was used for the transfer runs (5th run of the each session) but no feedback was presented.*

Training runs with contingent feedback were interspersed with "transfer runs" in which the patients were asked to down-regulate the ROIs without the aid of the feedback and by using the mental strategy learned during the neurofeedback training. Transfer runs were included in order to help subjects to self-regulate in a real-world environment (outside the scanner).

Brain data was analyzed in real-time with a commercially available software (Turbo-BrainVoyager-3.0 Brain Innovation, Maastricht, The Netherlands; Goebel, 2001), performing on-line incremental 3D motion detection and correction, and drift removal. The software is capable of incrementally computing statistical maps based on the General Linear Model (GLM) and event-related averages. The visual feedback ("monetary reward") was calculated from brain activity using Matlab 2012b (The MathWorks, Natick, MA) software running on a separate computer connected via local area network (LAN) to the scanner and to the Turbo-Brain Voyager (Caria et al., 2007).

During training sessions, eye-tracker recordings (SR-Research, Eyelink 1000) were collected to evaluate whether patients were attending and look up to the presented pictures during baseline and down regulation blocks, and if so, their pupil coordinates during the presentation of each picture. Furthermore, patients' pupil size changes during baseline and down-regulation blocks were measured by the eye-tracker device to investigate if pupil size could be an indicator of the OCD related sympathetic-parasympathetic activity.

Patients completed the State-Trait Anxiety Inventory (STAI-State) before and after each session as a measurement of current anxiety related to the fMRI measurement (Spielberger & Sydeman, 1994).

MR acquisition

MRI scans were acquired using a 3.0 Tesla body scanner, with standard 12-channel head coil (Siemens Magnetom Tim TRIO, Siemens, Erlangen, Germany) at the Dept. of Psychiatry, University of Marburg. A standard echo-planar imaging sequence was used for functional images (EPI; TR: 1.5 s, TE: 30 ms, matrix size: 64x64, flip angle α: 90°). Each volume consisted of 16 axial slices (voxel size: 3.3 x 3.3 x 5.0 mm^3, slice gap of 1 mm) in AC-PC alignment. In order to superimpose functional maps on brain anatomy, a high-resolution T1-weighted structural scan was collected in each session (MPRAGE, matrix size: 256 x 256, 176 sagittal slices, 1mm^3 isotropic voxels, TR= 1900 ms, TE: 2.52 ms, TI: 900 ms, flip angle α: 9°).

Offline analysis

Hypothesis driven ROI analysis was performed using the ROIs previously selected for each subject during the feedback training sessions. To evaluate the down-regulation performances of the participants, we compared BOLD signal level in the ROIs for every TR during the down-regulation blocks with the mean BOLD level during the previous baseline block. If the BOLD signal level in the down-regulation block was lower than the mean BOLD of the previous baseline block for that particular TR, it was counted as one "hit". Because each down-regulation block lasted 27 seconds (18 TR) and there were 6 blocks through one run, the maximum number of hits for one run could be 108. We counted every hit of every down-regulation block during the run and converted the total number of hits into the percentages.

Pre and Post behavioral tests

These tests were performed by each participant before and after the rtfMRI-BCI neurofeedback training.

1- Ecological Disgust Test (EDT)

The EDT was designed to evaluate each patient's response to a symptom provoking stimulus in a naturalistic environment. Outside the scanner and in a separate room, patients were shown real-world disgust inducing objects, selected individually for each patient according to his/her own self-reports during the screening session. The object was placed in the first position on a wheeled table at a distance of 5 meters apart from the patient. On the left side of this object, a clearly visible '+' sign and or a '↓' sign sign was shown. In each trial, the selected object was slowly brought towards the patient at a constant pace either with the '+' sign or with the '↓' sign. There were 20 trials of this kind, each sign being presented 10 times. Patients were instructed to focus on the object and say 'stop' when they feel that the object should not come any closer. As long as the patient does not say 'stop', the experimenter would move closer, and at the end bring the object in contact with the patient's hand. The distances between the starting point and the point at the "stop" moment were measured for '+' signed and '↓'

signed blocks along the direction of movement of the experimenter for both pre-test and post-tests. The meanings of the signs were not explained to the patients in the pre-test sessions. On the post-test, the same procedure and objects were used, but participants were instructed to use the cognitive strategies that they had learned during rtfMRI trainings. Thus, in the above tests, participants were instructed to recreate mental strategies that they had used during the neurofeedback training for the anterior insula down-regulation, but now in the absence of feedback and in real-life conditions.

Figure 2. *The Ecological Disgust Test and the flow of the experiment. The experimenter approached the patient with a real-life, disgust-inducing object from a distance of 5 meters either with a '↓' or '+' cue (10 times each). The patient focused on the object (two newly chewed gums in this picture) as the experimenter approached him/her, and said "stop" whenever he/she felt that the object should not come any closer. In the pre-test, the meanings of the cues are not explained to the patients. In the post-test, during down-arrowed runs, patients used the cognitive strategies that they had learned in the rtfMRI-BCI neurofeedback training sessions.*

2- Picture rating test:

We tested patient responses to disgust inducing pictures in a naturalistic environment, out of the scanner, using a set of visual contamination anxiety inducing stimuli, taken from the IAPS (Lang, Bradley & Cuthbert, 2008) and from several Internet sources. During the pre-test, 50 pictures (30 contamination anxiety related, 20 neutral-15 seconds each) were presented to the patients two times in two separate runs in a counterbalanced order via a 21.5" monitor. Patients were shown either a down arrow ('↓') or a plus sign ('+') on the right side of the screen attached to each picture. Pictures that were presented with the ('+') sign (baseline condition) in the first run were presented with the ('↓') sign (down-regulation condition) in the second run. The meanings of these signs were not explained to the patients in the pre-test. Patients were asked to rate the pictures after each presentation in three dimensions, i.e. valence, arousal and OCD-symptom provocation by using a visual analogue scale (VAS) (Gerich, 2007). The VAS scale was constructed as a line of 1680 mm length and the patients rated each picture with the help of the mouse in the aforementioned three dimensions. The positions of respondents' marks on the VAS were scaled as 1579 distinct points, resulting in codes from 1 to 1680. In the post-test, the same procedure was used, except for the fact that during the down-regulation conditions patients were instructed to use the cognitive strategies that they had learned in rtfMRI-BCI neurofeedback trainings.

Time ⟶

Figure 3. Picture-rating test. Patients rate each picture at the dimensions of valence, arousal and OCD symptom provocation. During the ratings, SCR and heart rate data were collected.

3- Physiological measures during picture ratings (SCR & HR)

Patients' physiological responses, i.e, skin conductance response (SCR) and heart rate (HR) were measured by a NeXus-32 Wireless Physiological Monitoring and Feedback System (Mind Media BV, The Netherlands) during the picture rating test. Skin conductance was measured from 2 electrodes attached to the palms of the non-dominant hand. Mean skin conductance levels were calculated for two conditions (disgusting picture-baseline, disgusting picture-down-regulation, 15 seconds each). Differences between baseline and down-regulation blocks in the pre- and post-tests were compared to assess the effects of rtfMRI-BCI neurofeedback training on the picture ratings. Heart rate variability (HRV) was monitored using a pulse oximeter. Inter beat intervals were converted to heart rate in beats per minute (BPM).

On the 8th, 9th and 10th days of the study (6th, 7th and the 8th days for the first two patients) the post–tests (EDT, picture rating, SCR/HR measurements) were performed.

After the post-tests, the assessment of the general psychopathology was performed again (as in pre-training clinical evaluation).

Results

In this section, we shall elaborate on the results of each patient's pre-test, rtfMRI-BCI neurofeedback training and post-test separately. We have chosen to present individual patient data instead of group data due to the small sample size of this pilot study.

Patients No. 1 and No. 2 participated for 2 days in the rtfMRI-BCI neurofeedback training (on the 4th and 5th days of their measurements) and continued with the post-tests on the 6th, 7th and 8th days, while patient 3 participated in four days of neurofeedback training and then continued with the post-tests on 8th, 9th and 10th days.

Patient 1

Patient 1 was a 19-year-old right-handed female. She was undergoing cognitive behavioral psychotherapy for 3 weeks during the measurements and was not using psychotropic medication. Patient's pre-post questionnaire results are presented in Table 2.

TEST	SCID I	Y-BOCs	FEE	BDI-II	STAI Trait	STAI State
Pre-test	F42.1 OCD, Predominantly compulsive acts	12	3.16	42	76	Pre-scan 69 Post-scan 68 Pre-scan 48 Post-scan 40
Post-test	-	11	1.68	-	-	

Table 2. *Clinical evaluation of the patient 1.*

According to SCID-I interview, Patient 1 met criteria for OCD with predominantly compulsive behavior. The Y-BOCs score also indicated mild OCD symptoms at the pre-test and post-test. The BDI-II indicated severe depression. In comparison to healthy subjects, the patient suffered from higher anxiety levels according to the STAI trait. According to FEE, Patient 1 showed elevated disgust sensitivity during the clinical assessment at the beginning of the experiment. After training, a decline in the disgust sensitivity was observed.

Real-time fMRI-BCI neurofeedback training analysis

Due to technical difficulties, the first patient could complete only two runs of rtfMRI-BCI training on the first day of rtfMRI-BCI neurofeedback training. As compared with the right insula, she show a more noticeable increase in the number of hits in the left insula across training sessions. On the second day, in the transfer run, the patient had 89 hits in the left insula, which corresponds to 82% of the possible total hits in a run. The patient used “thinking funny stories” as her cognitive strategy for down-regulation.

Figure 4. shows the percentage of the hits that Patient 1 achieved through rtfMRI-BCI neurofeedback training and the transfer runs from right anterior insula and left anterior insula respectively.

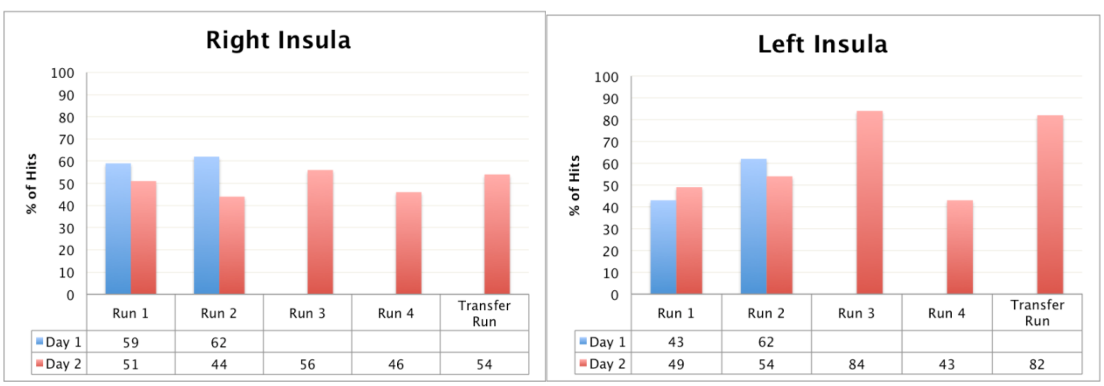

Figure 4. Percentage of the hits through rtfMRI-BCI neurofeedback training runs.

Heart rate measurements in the scanner

The first patient’s HR scores as bpm for baseline (M= 90.03, sd= 1.67) and down-regulation (M= 87.25, sd= 1.68) conditions on the first day of training were significantly different; $t(11)=5{,}528$, $p<0.01$. There was also a significant difference between baseline (M= 91.24, sd= 3.79) and down-regulation (M= 90.36, sd= 3.87) conditions in the second day of training; $t(23)=2.275$, $p<0.05$. In both days, HR was lower during the down-regulation blocks.

EDT

In the EDT, two newly chewed gums were used as real-life disgust objects. The distance between the starting point and the point at the "stop" moment were measured for '+' signed baseline and '↓' signed down-regulation blocks for both pre-test and post-tests. There was no significant difference between baseline and down-regulation conditions in pre-test in patient's response to the disgust object. However, we found a significant difference between baseline (M= 4.45 meters, sd= 0.32) and down-regulation (M= 4.89 meters, sd= 0.27) conditions in the post-test; $t(9)=-9.258$, $p<0.01$. During the down-regulation conditions the experimenter got closer to the patient with the disgust object. On 3 out of 10 post-test down-regulation trials, the patient allowed the experimenter to touch her hand with the chewed gum.

Picture ratings

The first patient's picture ratings in the dimensions of valence, arousal and symptom provocation showed no significant difference in the pre-test between baseline and down-regulation conditions. In the post-test, the difference between baseline and the down-regulation was significant for the valence and the symptom provocation dimensions. The patient rated the pictures as having less negative valence and less symptom provocation following the down-regulation blocks.

Test	**Measure**	**Baseline Ratings**	**Down-Regulation Ratings**	**T**	**df**
Pre-Test	Valence	1249.44 (334.99)	1250.380 (400.38)	.013	31
	Arousal	1021.094 (278.52)	1019.72 (301.67)	-0.022	31
	Sym. Prov.	1255.22 (395.37)	1255.97 (452.05)	0.010	31
Post-Test	Valence	1091.09 (252.62)	565.13 (290.50)	-8.839*	31
	Arousal	863.63 (227.95)	831.31 (223.29)	-0.708	31
	Sym. Prov.	954.28 (448.69)	190.63 (313.27)	-10.64*	31

Table 3. Means and standard deviations (in brackets) of disgust evoking picture ratings of the first patient.

Physiological measures during picture ratings (SCR & HR)

No statistically significant difference was observed in SCR between baseline (M=12.22, sd= 0.59) and down-regulation conditions (M=12.13, sd= .43) in the pre-test through the picture rating test. The differences between baseline (M=17.26, sd= 7.61) and down-regulation (M= 15.03, sd= 3.71) conditions did not reach significance in the post-test either.

HR differences between baseline (M= 88.49, sd= 2.13) and down-regulation (M=86.82, sd= 2.48) conditions in the pre-test were not significant. Also, no significant difference was observed between baseline (M=80.10, sd= 3.16) and down-regulation (M=79.79, sd=1.61) conditions in the post-test.

Patient 2

Patient 2 was a 25 years old right handed female. She was an in-patient, underwent cognitive behavioral psychotherapy for 3 weeks before the measurements and was using psychotropic medication (Setralin 150 mg). The patient's pre-post clinical results are presented in Table 4.

TEST	**SCID I**	**Y-BOCs**	**FEE**	**BDI-II**	**STAI Trait**	**STAI State**
Pre-test	F42.1 OCD, Predominantly compulsive acts.	6	2.16	0	51	Pre-scan 40 Post-scan 40
Post-test	-	9	2.92	-	-	Pre-scan 31 Post-scan 42

Table 4. *Clinical evaluation of the second patient.*

Patient 2 met SCID-I criteria for OCD predominantly with compulsive behavior, and had a low severity of symtomatology according to Y-BOCs. No clinically significant depression or anxiety was detected. Patient's disgust sensitivity and Y-BOCs score were slightly higher at the end of the experiment.

Real-time fMRI-BCI neurofeedback training analysis

The patient showed similar down-regulation performances on the first and the second days of the rtfMRI-BCI neurofeedback trainings. On the first day, she achieved 65 hits (60%) and 71 hits (65%) in the down-regulation of the right and the left insula, during the transfer runs respectively. On the second day, the number of hits from the right insula decreased to 56-(51%) but an increase was observed for the activations in the left insula (75 hits-69%).

The patient reported "thinking herself lying on the grass" as her cognitive strategy for down-regulation conditions.

Figure 5. displays the percentage of the hits that patient had through rtfMRI-BCI neurofeedback training and the transfer runs from right anterior insula and left anterior insula respectively.

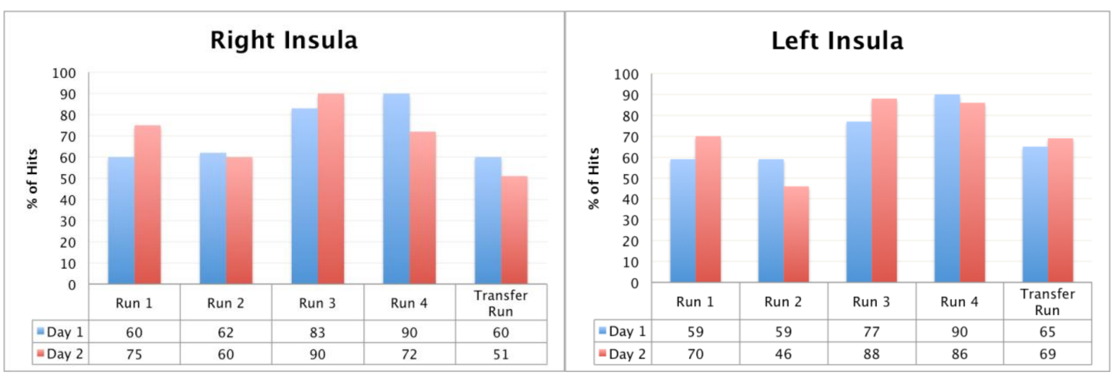

Figure 5. *Percentage of the hits through rtfMRI-BCI neurofeedback training runs.*

Heart rate measurements in the scanner

Patient's scores for baseline (M= 82.20, sd= 1.46) and down-regulation (M= 80.97, sd= 2.25) conditions on the first day of training were significantly different; $t(23)=2.692$, $p<0.05$, i.e. in the down-regulation condition, patient showed lower HR. On the second day of training, although the patient continued to show a slower HR in the down-regulation condition, the difference between the baseline (M= 93.76, sd= 2.79) and the down-regulation (M= 92.92, sd= 2.66) conditions did not reach significance.

EDT

In the EDT trials, used toilet papers from a toilet bin inside a nylon bag were used as disgust objects. The nylon bag's mouth was left open. The difference between baseline (M= 4.84 meters, sd= 0.11) and down-regulation (M= 4.85 meters , sd= 0.05) conditions in the pre-test did not reach significance. Likewise, no significant difference between baseline (M= 4.64 meters, sd= 0.07) and regulation (M= 4.67 meters, sd= 0.05) conditions was found in the post-test.

Picture rating test

The picture ratings of the second patient did not show any difference between the baseline and the down-regulation conditions both for pre- and the post-tests. Table 5. displays the overall results.

Test	**Measure**	**Baseline Ratings**	**Down-Regulation Ratings**	**t**	**df**
Pre-Test	Valence	1653.73 (266.14)	1673.10 (319.09)	0.450	29
	Arousal	945.4 (413.86)	1020.97 (445.48)	0.681	29
	Sym. Prov.	1011.033 (605.53)	1058.83 (624.35)	0.493	29
Post-Test	Valence	1478.7 (308.88)	1503.23 (285.81)	0.352	29
	Arousal	848.567 (335.70)	786.17 (277.62)	-1.173	29
	Sym. Prov.	1307.33 (562.27)	1291.17 (592.73)	-0.247	29

Table 5. *Means and standard deviations (in brackets) of disgust evoking picture ratings of the second patient.*

Physiological measures during picture ratings (SCR & HR)

The difference in SCR between the baseline (M= 4.83, sd= 0.9) and the down-regulation (M=5.21, sd= 0.98) conditions was significant in the pre-test (p= 0.013). SCR was higher during down-regulation conditions. In the post-test SCR differences between the baseline (M= 2.66, sd= 0.51) and the down-regulation (M= 2.56, sd= 0.63) conditions were not significantly different.

HR difference between baseline (M= 81.89, sd= 4.24) and the down-regulation (M= 81.84, sd= 3.60) in the pre-test was not significant but we found a significant difference between the conditions in the post-test (p=0.013). HR was higher in the down-regulation (M=90. 73, sd= 3.25) condition as compared with the baseline (M= 89.36, sd= 2.43).

Patient 3

The third patient was a 26 year old left handed male. He was under psychotropic medication

(Setralin 125 mg., Risperdal 0.5 mg.) but not participating psychotherapy during the measurements. Patient's pre-post questionnaire results are presented in Table 6. This patient received 4 days of rtfMRI-BCI neurofeedback training.

TEST	SKID I	Y-BOCS	FEE	BDI-II	STAI Trait	STAI State
Pre-test	F42.2 *OCD, Mixed obsessional thoughts and acts. *Major Depression	36	2.59	35	79	Pre-scan 57 Post-scan 57 Pre-scan 54 Post-scan 55 Pre-scan 65 Post-scan 55 Pre-scan 60 Post-scan 53
Post-test	-	33	3.08	-	-	

Table 6. Clinical evaluation of the third patient.

Patient 3 meet criteria for OCD and major depression. This is in accordance with BDI-II and Y-BOCs. A decrease in the Y-BOCs score was observed after training. Patient 3 showed high levels of anxiety before and during the experiments. The disgust sensitivity measured by FEE increased at the end of the experiments.

Real-time fMRI-BCI neurofeedback training analysis

The third patient showed a better down-regulation performance on the right insula compared with the other patients. He showed his best performance on the second day of trainings on the right insula.

As the mental strategy for the down-regulation, the patient mentally replaced the "ugly" parts in the pictures with "nicer" objects. On the third day of training the patient changed his strategy through the runs (e.g., thinking on nice memories, concentrating on colors of the objects). In this session, his overall number of hits was the lowest as compared with the other days.

Figure 6. displays the percentage of the hits that patient had through rtfMRI-BCI neurofeedback training and the transfer runs for four days.

Figure 6. *The percentage of the hits from the right and the left anterior insula respectively.*

Heart rate measurements in the scanner

In contrast to the previous two patients, the third patient showed increased HR during the down-regulation conditions as compared to the baseline through the rtfMRI-BCI neurofeedback training sessions. On the first day of the training, the scores for baseline (M= 72.89, sd= 1.26) and down-regulation (M= 73.89, sd= 1.64) conditions were significantly different; $t(17)=-2.359$, $p<0.05$. There was also a significant difference between baseline (M= 78.51, sd= 1.87) and down-regulation (M= 79.21, sd= 2.19) conditions on the second day of trainings; $t(23)=-2.536$, $p<0.05$. For the third day, no significant difference was found between baseline (M= 79.43, sd= 1.98) and regulation (M= 80.21, sd= 2.24) conditions. Likewise, there was no significant difference between baseline (M= 83.45, sd= 3.25) and regulation (M= 83.91, sd= 3.69) conditions on the fourth day.

EDT

For this patient, used toilet papers were the real-life disgust objects (similar to that of the second patient). These disgust objects were put into a nylon bag and the nylon bag's mouth was left open. The difference in patient's response between baseline (M=4.25 meters, sd=0.10) and down-regulation (M=4.27meters, sd=0.06) conditions in pre-test did not reach significance. There was a significant difference in the patient's response between baseline (M=4.26 meters, sd=0.13) and down-regulation (M=4.49 meters, sd=0.15) conditions in the post-test; $t(9)=-5.314$, $p<0.01$. The experimenter could get closer to the patient with the disgust object while the patient using his cognitive strategies during the down-regulation conditions.

Picture rating test

Patient's picture ratings showed no significant difference in the pre-test between baseline and down-regulation conditions in all three rating dimensions. In the post-test, the difference between the conditions was significant for the valence and the symptom provocation dimensions: the patient rated the pictures as less symptom provocative and having less negative valence in the post-test down-regulation conditions.

Table 7. shows the overall results.

Test	**Measure**	**Baseline Ratings**	**Down-Regulation Ratings**	**T**	**df**
Pre-Test	Valence	1862.80 (160.62)	1852.77 (117.55)	-0.298	29
	Arousal	1792.43 (235.26)	1717.27 (277.35)	-1.298	29
	Sym. Prov.	1720.53 (243.29)	1709.7 (295.10)	-0.237	29
Post-Test	Valence	1884.50 (95.76)	1825.33 (166.06)	-2.048*	29
	Arousal	1801.03 (212.57)	1747.93 (175.82)	-1.092	29
	Sym. Prov.	1708.07 (232.47)	1633.53 (240.25)	-2.295*	29

* p<0.05

Table 7. *Means and standard deviations (in brackets) of disgust evoking picture ratings of the third patient.*

Physiological measures during picture ratings (SCR & HR)

We didn't observe a statistically significant difference in the SCR between baseline (M= 1.43, sd= 0.18) and the down-regulation (M= 1.43, sd= 0.22) conditions in the pre-test. The difference between the conditions for the SCR in the post-test was not significant either (Baseline M= 1.39, sd= 0.31; Down-regulation M=1.42, sd= 0.28).

Also, HR difference between baseline (M= 81.96, sd= 4.94) and the down-regulation (M= 81.77, sd= 2.42) in the pre-test and post-test did not show any difference (Baseline M= 84.92, sd= 1.89; Down-regulation M=85.05, sd= 2.86).

Discussion

Recent evidence suggest that OCD with contamination obsessions and washing compulsions might be characterized by a disorder in disgust processing. The anterior insula hyperactivity may play a particularly important role in mediating such putative disruptions (Stein et al., 2006; Goetz et al., 2013; Starcevic et al., 2013). In light of these findings, we designed a pilot study to explore the effects of rtfMRI based anterior insula down-regulation on several behavioral, physiological and clinical measures of OCD patients with contamination fears and washing compulsions. Also, we aimed to examine the feasibility of our study procedures, validity of the tools and our overall approach that is intended to be used in a larger future study. Yet a further purpose was to introduce/present our methods, some of which were used for the first time (e.g., Ecological Disgust Test) in rtfMRI-BCI studies.

Our results show for the first time that anterior insula down-regulation is possible in OCD patients. In fact, all three patients could learn to decrease the BOLD signal in the anterior insula albeit to different degrees, in the presence of disgust inducing stimuli with rtfMRI-BCI. In operant conditioning, the success in learning a new behavior is determined by the contingency of the behavior-consequence associations. In rtfMRI-BCI experiments, the association between a mental strategy that successfully regulates a neural signal (behavior) and feedback (consequence) can be affected by the temporal delay of the feedback signal (Caria et al., 2011). In the great majority of rtfMRI studies, feedback is continuously presented with minimal delay, approximately around 2 seconds (Sulzer et al., 2013). Because the anterior insula displays strong functional connectivity with the anterior cingulate and because of its role in feeling and motivation (Craig, 2009), to prevent a possible activity increase in the insula due to reward processing itself, we averaged and presented the neurofeedback information to the patients at the end of each down-regulation block in our design, in line with some previous rtfMRI studies (Bray et al., 2007; Posse et al., 2003; Shibata et al., 2011; Yoo and Jolesz, 2002). By doing this the neurofeedback signal provided information about the monetary reward. Some studies however have suggested that intermittent feedback might be a better way to achieve a particular behavior – consequence association when mental imagery was used during self-regulation (Yoo & Jolesz, 2002; Johnson et al., 2012,) Hence, in a future study, it might be useful to provide patients about their ongoing brain activity at shorter intervals, e.g., every ten seconds (three times throughout each down-regulation block). To avoid cognitive or visual distractions, which can be caused by the presence of the graphical thermometer next to the disgust inducing pictures in the screen, it would be beneficial to locate each picture inside a frame which can provide neurofeedback, for example by color changes. In this manner it would be possible to separate the neurofeedback information from the reward, which will be presented at the end of each block.

In addition, the target regions selected for self-regulation and the self-regulation direction (either up or down) are crucial aspects in brain self-regulation experiments. The majority of previous rtfMRI studies used single ROI up-regulation paradigms in which participants had been trained to increase activity of one target region (for reviews please see Ruiz et al., 2013; Birbaumer et al., 2013; Sulzer et al., 2013). Up to now, fewer rtfMRI studies showed that subjects could learn to down-regulate the brain activity e.g., in amygdala (Brühl et al., 2014), subgenual anterior cingulate (Hamilton et al., 2011), auditory cortex (Haller, Birbaumer, and Veit 2010), anterior cingulate cortex (Li et al., 2012) and anterior insula (Caria et al., 2010; Veit et al., 2012; Li et al., 2012). Decreasing the BOLD activity might be harder as compared to increasing both in healthy and patient populations, although it might not be physiologically impossible as suggested by Logothetis and colleagues (2006). The above study showed negative BOLD responses correlate with reduction of neural activity in the attended regions. Our preliminary results are important in showing the possibility of down-regulation of an abnormally activated brain region in psychiatric populations. However, because OCD affects a distributed fronto-striatal circuit, a connectivity-based or a pattern classifier-based neurofeedback study design, instead of a single ROI design, might be an interesting possibility for future experimental designs. In a recent study, Weygandt and colleagues (2013) investigated whether fear, disgust and neutral emotional states can be decoded from brain patterns of fMRI information in OCD patients and healthy controls. Their results indicated that fMRI data contains information about OCD-relevant fear stimuli and by this information it is possible to distinguish between OCD patients and healthy controls. These results suggest that the requirements are met to conduct a future rtfMRI paradigm for the treatment of OCD using classifier-based neurofeedback. Indeed, these findings can be beneficial for a classifier-based up-regulation study.

Regarding the transfer runs, included to evaluate whether subjects could regulate anterior insula in absence of feedbacks, patients were less successful in self-regulation as compared with the regular training runs. Hence, improving the self-regulation ability in the absence of a real-time feedback with a design that includes more transfer runs would be crucial for future experiments, in order to improve the behavioral results measured outside the scanner environment

As a pilot study with 3 patients, it is not possible to reach generalize conclusions regarding the behavioral effects of rtfMRI-BCI neurofeedback training and related symptomatological changes. In fact, behavioral and clinical effects of the rtfMRI-BCI neurofeedback training were not consistent in all patients. Two of the three patients of the study (patient 1 and patient 3) showed improvements in the EDT, picture rating test and the clinical assessments achieved by questionnaires. However, patient 2 did not display any improvement in these dimensions.

In two cases, patients improved their capability to bear the physical proximity of a real-world disgusting symptom-provoking object, using their learned cognitive strategies for down-regulation after the training. Showing the application of the learned brain self-regulation to the real-life conditions, these results are encouraging for the rtfMRI-BCI neurofeedback studies as most of the previous studies focused on immediate changes in the behaviors or symptoms happening inside the scanner environment (Caria et al., 2010; Sitaram et al 2012; Ruiz et al., 2013; Buyukturkoglu et al., 2013). In that manner, novel symptom-specific tests, like EDT, would be important to explore the transfer of learned slef-regulation skills to “real-world” environments.

In parallel with the EDT results, the same two patients also showed improvements in the picture rating test in two dimensions i.e., valence and OCD symptom provocation. During the post-tests, patients rated the disgust evoking pictures with less negative valence and as less symptom provocative following down-regulation blocks.

Although patient 2 performed well during the rtfMRI-BCI neurofeedback training, she did not show any improvement in the behavioral or clinical measures. In fact, the patient's Y-BOCs scores were higher at the end of the experiments. Because the questionnaires used as clinical measures are self-administered and because we do not ask patients to use their mental strategies during the administration of the questionnaires, it is not possible to be certain whether the positive or negative changes in the scores could be attributed to the rtfMRI-BCI neurofeedback training, or to other factors active during this period.

Non-consistent results were observed for HR measures collected inside the scanner. Two patients (patient 1 and patient 2), displayed decreased heart rates during the down-regulation conditions. However, patient 3 had higher heart rates while down-regulating through the runs. HR measures, recorded while the patients were looking to the disgust inducing pictures outside the scanner, did not reveal a significant difference between the baseline and the down-regulation conditions in the post-tests in all three patients.

Previous psycho-physiological investigations exploring responses towards disgust inducing stimuli are limited in number and provide conflicting results, including heart rate. Although some studies show elevated HR in the conditions when healthy subjects are presented with symptom provoking pictures (Lang, Bradley, & Cuthbert, 1997; Alaoui-Ismaili et al., 1997; Schienle et al., 2001; Vrana, 1994), others point to a deceleration in the HR as an indicator of parasympathetic activity (Gross, 1998; Gross & Levenson, 1993; Johnsen, Thayer, & Hugdahl, 1995; Levenson, 1992). Studies that have measured OCD patients' physiological responses towards disgust inducing stimuli reported contradictory results as well. While some experimenters found elevated autonomic nervous system activity and HR (Benkelfat et al., 1991; Insel, Zahn, & Murphy, 1985; Rabavilas, Boulougouris, & Stefanis, 1977; Stein et al., 2006), other studies reported HR decelerations which is interpreted as a sign of orientation and not avoidance or stimulus rejection (Hoehn-Saric, McLeod, & Hipsley, 1995; Hollander et al., 1991; McCarthy, Ray, & Foa, 1995; Zahn, Leonard, Swedo, & Rapoport, 1996). One of the reasons for these conflicting findings might be the type of the stimuli used in the experiments. While the disgust emotion elicited in relation to contamination and pollution (e.g., pictures of dirty toilets, cockroaches, maggots on food, foul smells, facial expressions of expelling food), is characterized by HR acceleration, disgust elicited in relation to mutilation, injury and blood (e.g., injections, mutilation scenes, bloody injuries), seems to be characterized by a pattern of HR deceleration (Olantuji et al., 2013). In our set of stimuli we included both contamination and mutilation types of images. Therefore, and depending on the heterogeneity of the OCD patients, using both kind of pictures together in the same measurement might cause a neutralizing effect in HR measures. The differences on anxiety levels in our small group of patients might have also contributed to this inconsistency in HR results. Patient 3, who showed elevated HR during the down-regulation conditions in the scanner, showed also the highest anxiety level (both in trait and state-anxiety measures). Patients' elevated HR during down-regulation conditions might be also attributed to a high performance anxiety and reward expectancies.

Disgust is consistently reported to be associated with increased electrodermal activity (Olantuji et al., 2013). However, we did not observe a significant difference between disgust provoking and neutral pictures and skin conductance response levels. There were no significant differences in levels between baseline and down-regulation blocks while patients were viewing disgust inducing pictures either. Because we measured the mean skin conductance levels throughout baseline and the down-regulation blocks, these results might be due to the presentation of mixed type of disgust inducing pictures.

Because avoidance is a frequently observed response of the OCD patients (Starcevic et al., 2013), we wanted to be sure that the participants in the current study were consistently observing the presented pictures through the measurements. Inside the scanner, and through the rtfMRI-BCI trainings, we used an eye-tracker system for this purpose. The eye tracker system measured pupil location coordinates and size changes during the presentation of each picture. The preliminary analysis of eye tracker data confirmed that every patient of the study looked directly at the disgust inducing images throughout the runs. Apart from the sympathetic-parasympathetic effects on the pupil size and eye-blinks, these measurements are essential for future studies to ensure that patients observe the stimuli presented to them despite their highly disturbing nature.

In summary, in this pilot study we investigated the application of rtfMRI-BCI neurofeedback for anterior insula regulation in OCD patients. We also explored the feasibility of several behavioral and physiological pre and post-training tests and clinical assessments that would be used in a future long-term study. Our results indicate that with sufficient training OCD patients can learn to down-regulate the BOLD activity in their anterior insula in the presence of disgust inducing stimuli. The two tests that were designed to examine the effect of this self-control in real-world conditions outside the scanner (picture rating tests and the EDT) have important implications for future studies.

To improve the consistency of self-regulation, it might be crucial to combine rtfMRI-BCI neurofeedback sessions with extended neurofeedback training outside the scanner using portable EEG and/or functional near infrared spectroscopy (fNIRS). For this purpose, it would be useful to identify the EEG and/or fNIRS correlates of down-regulation of the BOLD signal anterior insula in each patient.

References

Alaoui-Ismaili, O., Robin, O., Rada, H., Dittmar, A., & Vernet-Maury, E. (1997). Basic emotions evoked by odorants: comparison between autonomic responses and self-evaluation. Physiology & Behaviour, 62, 713–720.

Aouizerate B, Guehl D, Cuny E, Rougier A, Bioulac B, et al. (2004). Pathophysiology of obsessive-compulsive disorder: a necessary link between phenomenology, neuropsychology, imagery and physiology. Prog Neurobiol 72:195–221.

APA – American Psychiatric Association. (2000). Diagnostic and Statistical Manual of Mental Disorders – DSM-IV-TR (4th edition, Text Revision). Washington, D.C.: American Psychiatric Association.

Beck AT, Ward CH, Mendelson M, Mock J, Erbaugh J. An inventory for measuring depression. Arch Gen Psychiatry. 1961;4:561-571.

Benkelfat, C., Mefford, I. N., Masters, C. F., Nordahl, T. E., King, A. C., Cohen, R. M., et al. (1991). Plasma catecholamines and their metabolites in obsessive-compulsive disorder. Psychiatry Research, 37(3), 321–331.

Birbaumer N, Cohen LG. (2007). Brain-computer interfaces: communication and restoration of movement in paralysis. J Physiol. 2007 Mar 15;579(Pt 3):621-36

Birbaumer N, Ruiz S, Sitaram R. (2013). Learned regulation of brain metabolism. Trends Cogn Sci. Jun;17(6):295-302.

Bray, S., Shimojo, S., O'Doherty, J.P., 2007. Direct instrumental conditioning of neural activity using functional magnetic resonance imaging-derived reward feedback. J. Neurosci. 27 (28), 7498–7507.

Broderick J, Grisham JR, Weidemann G. (2013). Disgust and fear responding in contamination-based obsessive-compulsive disorder during pictorial exposure. Behav Ther. Mar;44(1):27-38. doi: 10.1016/j.beth.2012.05.005. Epub 2012 Jun 8.

Brühl AB, Scherpiet S, Sulzer J, Stämpfli P, Seifritz E, Herwig U. (2014). Real-time neurofeedback using functional MRI could improve down-regulation of amygdala activity during emotional stimulation: a proof-of-concept study. Brain Topogr. Jan;27(1):138-48. doi: 10.1007/s10548-013-0331-9. Epub 2013 Nov 16.

Buyukturkoglu, K., Rana, M., Ruiz, S., Hackley, S. A. , Soekadar, S. R., Birbaumer, N., Sitaram, R.(2013). Volitional Regulation of the Supplementary Motor Area with fMRI-BCI neurofeedback in Parkinson’s disease: A Pilot Study. Conference Proceeding. Neural Engineering (NER), 6th International IEEE/EMBS Conference on 6-8 Nov 2013. San Diego, CA. Page(s): 677 – 681

Caria, A., Sitaram, R., Birbaumer, N., 2012. Real-time fMRI: a tool for local brain regulation. Neuroscientist 18 (5), 487–501.

Caria, A., Sitaram, R., Veit, R., Begliomini, C., Birbaumer, N., 2010. Volitional control of anterior insula activity modulates the response to aversive stimuli. A real-time functional magnetic resonance imaging study. Biol. Psychiatry 68 (5), 425–432.

Caria, A., Veit, R., Sitaram, R., Lotze, M., Weiskopf, N., Grodd, W., Birbaumer, N., 2007. Regulation of anterior insular cortex activity using real-time fMRI. NeuroImage 35 (3), 1238–1246.

Cisler, J. M., Olatunji, B. O., & Lohr, J. M. (2009). Disgust, fear, and the anxiety disorders: A critical review. Journal of Anxiety Disorders, 29(1), 34–46.

Craig, B., (2011). How do you feel - now? The anterior insula and human awareness. Nat. Rev. Neurosci. 10, 59–70.

Goebel, R., 2001. Cortex-based real-time fMRI. Neuroimage 13, S129.

Goodman WK, Price LH, Rasmussen SA, Mazure C, Fleischmann RL, et al. (1989) The Yale-Brown Obsessive Compulsive Scale. I. Development, use, and reliability. Arch Gen Psychiatry 46: 1006–1011.

Gross, J. J. (1998). Antecedent- and response-focused emotion mregulation: Divergent consequences for experience, expression, and physiology. Journal of Personality and Social Psychology, 74(1), 224–237.

Gross, J. J., & Levenson, R. W. (1993). Emotional suppression: Physiology, self-report, and expressive behavior. Journal of Personality and Social Psychology, 64(6), 970–986.

Haller, S., Birbaumer, N., Veit, R., 2010. Real-time fMRI feedback training may improve chronic tinnitus. Eur. Radiol. 20 (3), 696–703.

Hamilton, J.P., Glover, G.H., Hsu, J.J., Johnson, R.F., Gotlib, I.H., 2011. Modulation of subgenual anterior cingulate cortex activity with real-time neurofeedback. Human Brain Mapping. 32 (1), 22–31

Hoehn-Saric, R., McLeod, D. R., & Hipsley, P. (1995). Is hyperarousal essential to obsessive compulsive disorder? Diminished physiologic flexibility, but not hyperarousal, characterizes patients with obsessive-compulsive disorder. Archives of General Psychiatry, 52(8), 688–693.

Hollander, E., DeCaria, C., Nitescu, A., Cooper, T., Stover, B., Gully, R., et al. (1991). Noradrenergic function in obsessive-compulsive disorder: behavioral and neuroendocrine responses to clonidine and comparison to healthy controls. Psychiatry Research, 37(2), 161–177.

Insel, T. R., Zahn, T., & Murphy, D. L. (1985). Obsessive–compulsive disorder: an anxiety disorder. In: A. T. Tuma, & J. Maser (Eds.), Anxiety and the anxiety disorders (pp. 577–589). Hillsdale, NJ: Lawrence Erlbaum & Associates.

Johnsen, B. H., Thayer, J. F., & Hugdahl, K. (1995). Affective judgment of the Ekman faces: A dimensional approach. mJournal of Psychophysiology, 9(3), 193–202.

Johnson, K.A., Hartwell, K., LeMatty, T., Borckardt, J., Morgan, P.S., Govindarajan, K., Brady, K., George, M.S., 2012. Intermittent "real-time" fMRI feedback is superior to continuous presentation for a motor imagery task: a pilot study. J. Neuroimaging 22 (1), 58–66.

Lang, P. J., Bradley, M. M., & Cuthbert, B. N. (1997). Motivated attention: affect, activation, and action. In: P. J.

Lang, R. F. Simons, & M. Balaban (Eds.), Attention and orienting: sensory and motivational processes (pp. 97–135). Hillsdale, NJ: Lawrence Erlbaum Associates.

Lang, P. J., Bradley, M. M., & Cuthbert, B. N. (2005). International affective picture system (IAPS): affective ratings of pictures and instruction manual. Technical report A-6. Gainesville, FL: Center for Research in Psychophysiology, University of Florida.

Levenson, R. W. (1992). Autonomic nervous system differences among emotions. Psychological Science, 3(1), 23–27.

Li, X., Hartwell, K.J., Borckardt, J., Prisciandaro, J.J., Saladin, M.E., Morgan, P.S., Johnson, K.A., LeMatty, T.,

Brady, K.T., George, M.S., 2012. Volitional reduction of anterior cingulate cortex activity produces decreased cue craving in smoking cessation: a preliminary real-time fMRI study. Addict. Biol.

Linden, D. E., Habes, I., Johnston, S. J., Linden, S., Tatineni, R., Subramanian, L., Sorger, B., Healy, D., & Goebel, R. (2012). Real-time self-regulation of emotion networks in patients with depression. PLoS ONE, 7, e38115.

Mataix-Cols, D., Wooderson, S., Lawrence, N., Brammer, MJ., Speckens, A., Phillips, ML. (2004). Distinct neural correlates of washing, checking, and hoarding symptom dimensions in obsessive-compulsive disorder. Arch Gen Psychiatry. 61(6):564-76.

McCarthy, P. R., Ray, W. J., & Foa, E. B. (1995). Cognitive influences on electrocortical and heart rate activity in obsessive-compulsive disorder. International Journal of Psychophysiology, 19(3), 215–222.

Menzies L, Chamberlain SR, Laird AR, Thelen SM, Sahakian BJ, Bullmore ET. Integrating evidence from neuroimaging and neuropsychological studies of obsessive-compulsive disorder: the orbitofronto-striatal model revisited. Neurosci Biobehav Rev. 2008;32(3):525-549.

Millet B, Dondaine T, Reymann JM, Bourguignon A, Naudet F, Jaafari N, Drapier D, Turmel V, Mesbah H, Vérin M, Le Jeune F. (2013). Obsessive compulsive disorder networks: positron emission tomography and neuropsychology provide new insights. PLoS One.;8(1):e53241.

Moretz, M.W., McKay, D. (2008). Disgust sensitivity as a predictor of obsessive-compulsive contamination symptoms and associated cognitions. J Anxiety Disord. 22(4):707-15.

Muris P, van der Heiden S, Rassin E. (2008). Disgust sensitivity and psychopathological symptoms in non-clinical children. J Behav Ther Exp Psychiatry. 2008 Jun;39(2):133-46. Epub 2007 Mar 12.

Olatunji BO, Davis ML, Powers MB, Smits JA. (2013). Cognitive-behavioral therapy for obsessive-compulsive disorder: a meta-analysis of treatment outcome and moderators. J Psychiatr Res. Jan;47(1):33-41.

Olatunji, B. O., Cisler, J. M., Deacon, B. J., Connolly, K., & Lohr, J. M. (2007). The disgust propensity and sensitivity scale-revised: Psychometric properties and specificity in relation to anxiety disorder symptoms. Journal of Anxiety Disorders, 21, 918–930.

Olatunji, B. O., Sawchuk, C. N., Lohr, J. M., & de Jong, P. J. (2004). Disgust domains in the prediction of contamination fear. Behaviour Research and Therapy, 42(1), 93–104.

Phillips, ML., Marks, IM., Senior, C., Lythgoe, D., O'Dwyer, AM., Meehan, O., Williams, SC., Brammer, MJ., Bullmore, ET., McGuire, PK. (2000). A differential neural response in obsessive-compulsive disorder patients with washing compared with checking symptoms to disgust. Psychol Med. 30(5):1037-50.

Posse, S., Fitzgerald, D., Gao, K., Habel, U., Rosenberg, D., Moore, G.J., Schneider, F., 2003. Real-time fMRI of temporolimbic regions detects amygdala activation during single-trial self-induced sadness. NeuroImage 18 (3), 760–768.

Rabavilas, A. D., Boulougouris, J. C., & Stefanis, C. (1977). Synchrony and concordance on subjective and psychophysiological measures after beta-blockade and flooding in obsessive–compulsive patients. In: J. C.

Boulougouris, & A. D. Rabavilas (Eds.), The treatment of phobic and obsessive-compulsive patients (pp. 115–125). Oxford: Pergamon.

Rachman, S. (2004). Fear of contamination. Behaviour Research and Therapy, 42(11), 1227–1255.

Ruiz, S., Lee, S., Soekadar, S.R., Caria, A., Veit, R., Kircher, T., Birbaumer, N., Sitaram, R., 2013. Acquired self-control of insula cortex modulates emotion recognition and brain network connectivity in schizophrenia. Hum. Brain Mapp. 34 (1), 200–212.

Ruiz, S., Sitaram, R., Lee, S., Soekadar, S., Caria, A., Veit, R., Kircher, T., Birbaumer, N., Sitaram, R. (2011b). Acquired self-control of insula cortex modulates emotion recognition and brain network connectivity in schizophrenia. Human Brain Mapping.

Ruscio, AM., Stein, DJ., Chiu, WT., Kessler, RC. (2010) The epidemiology of obsessive-compulsive disorder in the National Comorbidity Survey Replication. Mol Psychiatry. 15 (1):53-63. Epub 2008 Aug 26.

Scheinost D, Stoica T, Saksa J, Papademetris X, Constable RT, Pittenger C, Hampson M. (2013). Orbitofrontal cortex neurofeedback produces lasting changes in contamination anxiety and resting-state connectivity. Transl Psychiatry. 2013 Apr 30;3:e250.

Schienle, A., Dietmaier, G., Ille, R., & Leutgeb, V. (2002). Eine Skala zur Erfassung der Ekelempfindlichkeit. Zeitschrift für Klinische Psychologie und Psychotherapie, 39, 80–86.

Schienle, A., Schäfer, A., Stark, R., Walter, B., Kirsch, P., & Vaitl, D. (2003). Disgust processing in phobia of blood–injection–injury: an fMRI study. Journal of Psychophysiology, 17, 87–93.

Schienle, A., Stark, R., & Vaitl, D. (2001). Evaluative conditioning: A possible explanation for the acquisition of disgust responses? Learning and Motivation, 32(1), 65–83.

Shapira, N. A., Liu, Y., He, A. G., Bradley, M. M., Lessig, M. C., James, G. A., Goodman, W. K. (2003). Brain activation by disgust-inducing pictures in obsessive-compulsive disorder. Biological Psychiatry, 54(7), 751–756.

Sitaram, R., Caria, A., Veit, R., Gaber, T. (2008a). Volitional control of insula using an fMRI Brain-Computer Interface in criminal psychopaths enhances functional connectivity of the emotional network. 38th annual meeting of the Society for Neuroscience, Washington

Sitaram, R., Lee, S., Ruiz, S., Rana, M., Veit, R., Birbaumer, N. (2010). Real-time support vector classification and feedback of multiple emotional brain states. Neuroimage. May 15;56(2):753-65.

Sitaram, R., Veit, R., Stevens, B., Caria, A., Gerloff, C., Birbaumer, N., Hummel, F. (2012). Acquired control of ventral premotor cortex activity by feedback training: an exploratory real-time FMRI and TMS study. Neurorehabil Neural Repair. Mar-Apr;26(3):256-65.
Spielberger CD, Gorsuch RL, Lushene RE. Manual for the State-Trait Anxiety Inventory. Palo Alto, CA: Consulting Psychologists Press; 1970.

Stein, D. J., Arya, M., Pietrini, P., Rapoport, J. L., & Swedo, S. E. (2006). Neurocircuitry of disgust and anxiety in obsessive-compulsive disorder: a positron emission tomography study. Metabolic Brain Disease, 21(2–3), 267–277.

Sulzer, J., Haller, S., Scharnowski, F., Weiskopf, N., Birbaumer, N., Blefari, M., Bruehl, A., Cohen, L., deCharms, R., Gassert, R., Goebel, R., Herwig, U., LaConte, S., Linden, D., Luft, A., Seifritz, E., Sitaram, R., 2013. Real-time fMRI neurofeedback: progress and challenges. Neuroimage 76, 386–399.

Tsao SD, McKay D. (2004). Behavioral avoidance tests and disgust in contamination fears: distinctions from trait anxiety. Behav Res Ther. Feb;42(2):207-16

Veit, R., Singh, V., Sitaram, R., Caria, A., Rauss, K., Birbaumer, N., 2012. Using real-time

Vrana, S. R. (1994). Startle reflex response during sensory modality specific disgust, anger, and neutral imagery. Journal of Psychophysiology, 8(3), 211–218.

Wright P, He G, Shapira NA, Goodman WK, Liu Y. (2004). Disgust and the insula: fMRI responses to pictures of mutilation and contamination. Neuroreport. Oct 25;15(15):2347-51.

Yoo, S.S., Jolesz, F.A., (2002). Functional MRI for neurofeedback: feasibility study on a hand motor task. Neuroreport 13 (11), 1377.

Zahn, T. P., Leonard, H. L., Swedo, S. E., & Rapoport, J. L. (1996). Autonomic activity in children and adolescents with obsessive-compulsive disorder. Psychiatry Research, 60(1), 67–76.

2. 2. Effect of motion correction algorithms on feedback in real-time fMRI (Submitted Manuscript)

Buyukturkoglu K, Rana M, Dietzsch L, Arikan B.E, Rana M, Ruiz S, Kircher T, Sitaram R, Birbaumer N, Roettgers H. Sommer J, (2014). (under revision). Frontiers in Neuroscience. Hosting Specialty: Frontiers in Behavioral Neuroscience, Research Topic Title: Learned brain self- regulation for emotional processing and attentional modulation: from theory to clinical applications. (Under revision).

Introduction:

Learning can be defined as a change in behavior that results from experience (Raygor, 2005; Klein, 2014). The modification of a certain behavior can be achieved by the use of positive and negative reinforcement through operant conditioning (Skinner, 1974; Sakurai et al., 2014). Effectiveness of the behavior-consequence association in operant conditioning/learning paradigms can be increased or decreased by various factors such as satiation/deprivation of the organism through training and immediacy (temporal contiguity), size or the contingency of the feedback (Schacter et al., 2011). Contingency refers to the conditional probability of reinforcement given a response or given a failure to respond (Sulzer et al., 2013). When a target response is not contingently (reliably, or consistently) followed by the consequence, effectiveness of the consequence upon the response is reduced (Schacter et al., 2011). However a consequence that follows the response consistently after successive instances would have profound effects upon the operant behavior (Ferster & Skinner, 1957).

In real-time functional magnetic resonance imaging (rtfMRI) neurofeedback studies, subjects are trained to control brain activity (a particular neural signal or a combination of neural signals) by operant conditioning when feedback and reward related to these signals are repeatedly presented to them (Weiskopf et al., 2007; Birbaumer et al., 2013; Ruiz et al., 2013). However, apart from the underlying neural activity, the noise from heart rate and respiration (Glover et. al., 2000; Noll & Schneider 1994; Hu et al., 2005), eye movements (Zhang et al., 2011) and head motion (Hajnal et al., 1994; Thacker et al., 1999; Cox and Jesmanowicz, 1999; Friston et al., 1996) may also modulate the signal from fMRI and rtfMRI. In particular, artifacts due to subject motion can degrade the fMRI signal, even if the motion is smaller than the fMRI voxel size (Oakes et al., 2005; Field et al., 2000; Sulzer et al., 2013). If the neurofeedback provided to the subjects is mainly based on physiological or movement artifacts instead of the underlying neural activity, it would disturb the behavior-consequence association and inhibit the self-regulation ability and the overall learning performance of the subject. Hence, to achieve efficient learning of brain self-control, a contingent feedback presented to the subjects by the rtfMRI system is crucial (Koush et al., 2012).

In contrast to conventional fMRI analyses with packages like SPM or FSL, in rtfMRI the time available for data pre-processing and statistical analysis is very limited. Therefore the processing pipeline includes only those steps that are considered to be essential and these are additionally optimized for data quality and speed. As subject motion would shift the brain and the region for feedback estimation, motion correction is an essential processing step.

Online motion correction can be performed prospectively or retrospectively. Prospective motion correction methods either capture the motions of the subject with an optical camera system or field sensors (McConnell et al., 1997; Eviatar et al., 1997; Zaitsev et al., 2006; Herbst et al., 2011; Andrews-Shigaki et al., 2009; Qin et al., 2009; Schulz et al., 2011; Forman et al., 2010; MacLaren et al., 2011; Weinhandl et al., 2010; Ooi et al., 2009) or use navigator echos of the MRI (van der Kouwe et al., 2006; Fu et al., 1995; Ward et al., 2000; Welch et al., 2002; White et al., 2010; Tisdall et al., 2012; Kober et al., 2011; MacLaren et al., 2011) to adjust the slice, phase and frequency encoding gradients for the measurement. Retrospective algorithms operate on the fully acquired data. They either use the raw data, i.e. handle k-space data (Lee et al., 2009; Lin et al., 2005, Lin W & Song H, 2009), or the final images. (Friston et al., 1996; Hu et al., 1994; Glover, Lee & Ress, 2000; Jenkinson et al., 2001; Caria et al., 2007; Mathiak & Posse, 2001; for detailed reviews see Oakes et al., 2005 and MacLaren et al., 2013).

In this study we tested the consistency of feedback calculated from data preprocessed with two retrospective real time motion correction algorithms. The first algorithm is included in the image reconstruction of the MRI scanner's EPI sequence (3d k-space interpolation, Advanced Retrospective Technique, Siemens, Erlangen, Germany) and operates on the raw data in k-space. The second uses the data after Fourier transformation, i.e. the images, and is included in Turbo Brainvoyager (TBV, Brain Innovation, Maastricht, The Netherlands). It is an iterative algorithm using trilinear interpolation. Both algorithms use 6 degrees of freedom, 3 for translation and 3 for rotation.

Under the assumption that both algorithms yield similar results, we expected a high correlation between the feedback values derived from the motion corrected data sets.

Methods:

This study was approved by the local ethics committees and all participants provided written consent for participating in this study.

Paradigm: 3 subjects (1 f, age 29.3 ± 4.0 years) were included in 2 (2 subjects) or 3 sessions of a neurofeedback training. Each session consisted of four runs with feedback and one run without feedback (transfer run). Each run included 6 trials with a duration of 60 seconds. During the first 30 seconds the subjects watched a picture stimulus (baseline, condition 1), then the picture stimulus changed and the subjects were asked to modulate their brain activity (regulation, 27 seconds, condition 2). All pictures showed disgusting scenes and were intended to induce an affective response. If the subject was able to change brain activity during the second condition, depending on the success of the self-regulation, a monetary reward/feedback was calculated and presented at the end of each trial (3 seconds). If the subject was not successful in self-regulation, a feedback with a “0 Euros” (Zero Euro) was presented.

Data acquisition: Data was acquired with a 3T MRI scanner (Tim Trio, Siemens, Erlangen, Germany) at the Dept. of Psychiatry, Marburg University, equipped with a standard 12 channel RX head coil. Scanning protocol for real time fMRI was based on the BOLD sensitive EPI sequence.

Scanning parameters: TR 1500ms, TE 30ms, FoV 192mm, 16 slices, 64x64 matrix, 5mm slice thickness, 20% gap, 90° flip angle, pixel bandwidth 2232Hz, phase encoding direction anterior-posterior, no parallel imaging. Retrospective motion correction using 3d k-space interpolation was turned on and raw data should also be stored (Raw, Figure 1), so that the system saved motion corrected images as an additional series (Siemens-MoCo, Figure 1, Siemens Advanced Retrospective Technique, ART). In total 250 volumes were acquired in each run. The first trial started with the 11th volume.

Feedback calculation: Dicom files were exported online from the MRI to a network drive (Figure 1, Real-time Analysis) and processed by TurboBrainVoyager 3.0 (TBV, BrainInnovation, Maastricht, The Netherlands) and an in-house plugin. We used Presentation (Neurobehavioral Systems, Berkeley, CA) as the software for the stimulus delivery.

Feedback was calculated in the plugin as:

with , i.e. the signal average of the regions of interest (ROI 1, 2 and 3), and C an arbitrary but fixed proportionality constant. A positive feedback value was achieved when brain activity was reduced during the second condition relative to the first condition.

For our paradigm with the presentation of affective stimuli, the active ROIs 1 and 2 were located in the left and right anterior insula, and the a reference ROI namely ROI3, to cancel out the effect of global activations located close to the parietal cortex (Figure 2). They were determined ahead of the first session based on a functional localizer. To ascertain an almost identical location of the ROIs over the sessions an auto alignment localizer was utilized for the slice positioning (Benner et al., 2006). Subject data and ROI sizes are summarized in Table 1.

During the experiments TBV motion corrected data (TBV-MoCo, trilinear interpolation) had been used to calculate the feedback. Offline analysis of the Siemens-MoCo data was done analogously by TBV and our in-house plugin. TBV-MoCo is part of the TBV package and is executed on the rtfMRI computer whereas Siemens-MoCo is included in the image calculation on the MRI scanner. Both algorithms assume a rigid body model and estimate the optimal motion correction parameters iteratively. They stop after reaching a predefined threshold for the difference between the actual and the reference image or after reaching the maximal number of iterative steps. The resulting image is either calculated with a trilinear interpolation (TBV-MoCo) or a 3d k-space interpolation (Siemens-MoCo).

Correlations:

Pearson correlation coefficients for the motion correction parameters (three translation parameters, three rotation parameters) from TBV and Siemens as well as for the feedback values based on TBV-MoCo and Siemens-MoCo data were calculated for each run (Figure 1, correlation test "between" motion correction algorithms.

Next, we additionally included an exponential moving average filter (EMA-filter) in the processing pipeline for TBV-MoCo and Siemens-MoCo data and calculated the reward parameter and the correlation with the unfiltered data (Figure 1, correlation test "within" motion correction algorithm and "between EMA" filtered data). Basic idea of the EMA filter is to calculate a filtered signal S_t from a time series y_t as $S_t = \alpha\ y_t + (1- \alpha)\ S_{t-1}$. Here we used an $\alpha = 0.97$ ($\alpha = \tau/(\tau+TR)$, TR of 1.5s and a filter parameter τ of 48.5s). Details on the use of EMA-filtering in rtfMRI are described in (Koush et al., 2012).

As a last step, we tested the effect of two outlier removal strategies. We calculated the average signal and standard deviation for each voxel. Voxel values above two standard deviations from the average were marked as outliers within its data series. Our first outlier removal method rejected these outliers from the ROI averages. The second outlier removal method counted the number of voxels identified as outliers within one time point (volume) and included only time points in the calculation where the number of rejected voxels was below a predefined threshold. Method 1 is sensitive to noise within individual voxels. Method 2 is sensitive to global changes (e.g. head motion). Using this data we calculated again the feedback parameters and the correlations 'within' and 'between' the pipelines. These correlations are not labeled in Figure 1, but follow the scheme of the EMA-filter.

To estimate the processing time of the pipelines, all data was post processed with one PC (CPU Core i7-3630, 2.4GHz, 8GB memory, 240GB OCZ Vertex 3 SSD, Windows 7 64 Bit) and timing information recorded.

Results:

Correlation of motion correction parameters:

Visual inspection of the motion corrected images did not show relevant remaining motion for either correction algorithm. The parameter curves in the time series (Figure 3a, smooth motion along z-direction, and 4a, several jumps) resemble each other in appearance. This impression is also supported by the correlation coefficients (r^2) in Table 2. We have to take into account that the absolute error of the estimated correction parameter does not depend on the amount of motion and therefore the relative error is systematically higher for small motions. As both algorithms worked overall fine this led to higher correlation coefficients for runs with more subject motion (see data ranges of scatter plots in Figures 3b, 4b). In general the Siemens-MoCo parameters are more fluctuating and are by trend bigger than the TBV-MoCo parameters.

Correlation of feedback parameter:

R^2 of the correlation coefficients for the feedback calculated from TBV-MoCo and Siemens-MoCo data are listed in Table 2 ("between").

Surprising is the high number of runs where the rewards calculated from TBV-MoCo data and Siemens-MoCo data are not highly correlated. r^2 is below 0.6 for 10 out of 35 runs. Figure 5 shows time series data and scatter plots of the third session from subject 3. As mentioned above, the correlation between two series of small values (e.g. Figure 5, run 3) is more error prone than between series including high feedback values when noise is of identical size for the data series. To identify whether the low correlation values were related to a single ROI or a subgroup of voxels (e.g. ROI edges) we drew time series plots of the ROIs (Figure 6) and voxel maps of the runs (Figure 7). In Figure 6 jumps in the z-translation parameter are associated with big changes in the ROI values. While most of the time ROI values do not differ between the two processing pipelines, we see a clear dissociation in the second run for the values of ROI 1 and 2 (Figure 5, trials 3-6). For this run the motion parameters from both algorithms are displayed in Figure 4a,b.

The EMA-filter did not improve the correlation between the two algorithms (Figure 1, "between EMA"). Still 10 out of 35 runs have an r^2 below 0.6. The correlation between the unfiltered and EMA-filtered data (Figure 1, "within TBV" and "within Siemens") was very high for both algorithms ($r^2 > 0.997$ for all runs), indicating only small changes in the data.

The first method of outlier removal resulted in an average rejection of 11 time points of the individual voxels but it didn't improve the correlation between the pipelines. In the second method we set the threshold to reject volumes to 12.5% of the voxels within the ROIs, i.e. for subject 1, 2 and 3 a volume was rejected when 8, 13 or

23 of the voxels within the ROIs were outliers. Correlation parameters and number of rejected volumes of method 2 are listed on the right hand side of Table 2.

All TBV timing information was estimated during post processing with identical data and ROIs but without saving TBV logfiles, i.e. RTP and BTC. Subsequently created files were deleted before the next analysis started. Read volume time was independent of other parameters around 40ms. Full volume time varied strongly between runs with (average 120ms, range 93 – 156ms) and without TBV motion correction (average 46ms, range 46-47ms). Our TBV-plugin required 600ms for saving unfiltered and filtered ROI data in ASCII-format at the end of each trial. EMA calculation for 188 voxels did not increase processing time (subject 3 with ROI sizes of 66 voxels (ROI 1 and 2) and 56 voxels (ROI 3)). The time needed by the MR imaging computer to create the DICOM files and write them to the network drive was not measured in this experiment.

Discussion:

The basic idea of neurofeedback with rtfMRI is to provide the subject with information about signal changes in the brain. This information should be related to the activity initiated by the subject, so the subject can realize the link between both and learn to control the signal change. While the way how the feedback value is associated with the MRI data varies between studies, the data preprocessing always includes some motion correction. In this study we tested the effect of two motion correction algorithms on the feedback. As our calculation included averaging over a long period of time and extended regions of interest, the temporal and spatial noise is smoothed out and we expected a good linear correlation of the results from the two preprocessing pipelines as long as the motion correction algorithms work fine.

We found however in more than 30 percent of the runs incongruent feedback value, i.e. the correlation between feedback calculated from TBV-MoCo data and feedback calculated from Siemens-MoCo data was low.

Especially feedback values around zero are prone to errors. This becomes obvious in subject 3, third run of the third session (Figure 5, run 3, trials 4-6). While one processing pipeline provides a positive feedback value, the other gives a negative value of the same size. This still happens when the absolute motion is small and the correlation of the motion correction parameters is high (Figure 6, run 3, trials 4+5 and Table 2). So even small differences between the two algorithms can give rise to a relevant difference in the feedback.

What does this mean for the subject? As we only gave positive feedback and omitted negative, our third subject would have received in 6 (TBV-MoCo) or 11 (Siemens-MoCo) out of 36 trials a positive feedback, just depending on the motion correction algorithm (Figure 5). This diminishes the enforcement strategy and leads to more training sessions.

To improve the correlation of the feedback values between the different MoCo algorithms, we tested an EMA-filter and two simple outlier removal strategies. The EMA-filter had little effect on the data and did not improve the correlation between the pipelines. The first outlier removal strategy (rejecting individual voxel data) worsened the results, but the second strategy (rejecting whole ROI data for individual time points) seems promising. Still we need to identify optimal parameters and we have to test the effect on different feedback estimations, i.e. continuous and/or intermittent feedback.

Right now, it is not obvious which pipeline provides better feedback, but wrong feedback information will increase the level of difficulty for the subject to identify an effective training strategy and can therefore prolong the training. Further studies should include simulations to decide on optimal data preprocessing.

A general question is related to the correlation analysis we used to identify the effects of different processing pipelines.

In theory any change to a data series becomes visible as a decreased correlation between the original and the modified data series. Here the initial data set is the measured signal in k-space. The two MoCo algorithms create two slightly different data sets. Noise from the measurement should be included in a similar way in both data sets. And it should be leveled out by the way how we calculate the feedback parameter, i.e. over several voxels (a minimum of 24 voxels for ROI 1 + 2 of the first subject, see Table 1) and time points (20 in condition 1 and 18 for condition 2). So the difference in the feedback is related to the processing pipelines and can be identified with a correlation analysis.

What can we learn about feedback quality? In signal processing basic concepts include filtering and artifact removal to improve data quality. Various implementations of these techniques are used in rtfMRI data processing. With the corresponding quality parameters we can describe their effects but there is no direct link to the feedback quality. Unfortunately we can only conclude from a low correlation between the two preprocessing pipelines that the feedback quality will be poor in at least one of them. From a high correlation between the pipelines we learn that the feedback parameter calculation is robust according to the processing pipelines, but this does not implicate a correct feedback.

Conclusion:

The results from our preliminary study suggest the feedback to be dependent on the motion correction algorithm. Restricting subject head movement remains a strong prerequisite for fMRI and rtfMRI experiments. But as even small movements lead to differences in the feedback, the robustness of the feedback parameter must be tested in future studies with respect to motion.

References:

Andrews-Shigaki BC, Armstrong BSR, Zaitsev M, Ernst T. Prospective motion correction for magnetic resonance spectroscopy using single camera retro-grate reflector optical tracking. J Magn Reson Imaging 2011;33:498–504.

Benner T, Wisco J, van der Kouwe AJW, Fischl B, Vangel MG, Hochberg FH, Sorensen AG. (2006). Comparision of Manual and Automatic Section Positioning of Brain MR Images, Radiology, Vol. 239, p246-254.

Birbaumer N, Ruiz S, Sitaram R. (2013). Learned regulation of brain metabolism. Trends Cogn Sci. Jun;17(6):295-302.

Caria, A., Veit, R., Sitaram, R., Lotze, M., Weiskopf, N., Grodd, W., Birbaumer, N. (2007). Regulation of anterior insular cortex activity using real-time fMRI. NeuroImage 35, 1238–1246.

Cox, R.W., Jesmanowicz, A., 1999. Real-time 3D image registration for functional MRI. Magn. Reson. Med. 42, 1014 – 1018.

Derbyshire JA, Wright GA, Henkelman RM, Hinks RS. Dynamic scan- plane tracking using MR position monitoring. J Magn Reson Imaging 1998;8:924–932.

Eviatar H, Saunders JK, Hoult DI. Motion compensation by gradient adjustment. In Proceedings of the 5th Annual Meeting of ISMRM, Vancouver, Canada, 1997. p. 1898.

Ferster, C. B. & Skinner, B. F. "Schedules of Reinforcement", 1957 New York: Appleton-Century-Crofts.

Field, A. S., Yen, Y. F., Burdette, J. H., & Elster, A. D. (2000). False cerebral activation on BOLD functional MR images: Study of low-amplitude motion weakly correlated to stimulus. American Journal of Neuroradiology, 21, 1388-1396.

Forman C, Aksoy M, Hornegger J, Bammer R. Self-encoded marker for optical prospective head motion correction in MRI. Med Image Comput Comput Assist Interv 2010; 13(pt 1):259–266.

Friston, K.J., Williams, S., Howard, R., Frackowiak, R.S.J., Turner, R., 1996. Movement-related effects in fMRI time series. Magn. Reson. Med. 35, 346 – 355.

Fu Z, Wang Y, Grimm R, Rossman P, Felmlee J, Riederer S, Ehman R. Orbital navigator echoes for motion measurements in magnetic resonance imaging. Magnetic Resonance in Medicine 1995; 34:746–753.

Glover, G.H., Li, T.Q., Ress, D. (2000). Image-based method for retrospective correction of physiological motion effects in fMRI: RETROICOR. Magn. Reson. Med. 44, 162–167.

Hajnal, J.V., Myers, R., Oatridge, A., Schwieso, J.E., Young, I.R., Bydder, G.M., 1994. Artifacts due to stimulus correlated motion in functional imaging of the brain. Magn. Reson. Med. 31, 283 – 291.

Herbst M, Maclaren J, Korvink JG, Zaitsev M. A practical tracking system to avoid motion artifacts. In Proceedings of the 19th Annual Meeting of ISMRM, Montreal, Canada, 2011. p. 2683.

Hu X, Kim SG. Reduction of signal fluctuation in functional MRI using navigator echoes. Magn Reson Med 1994; 31:495–503.

Jenkinson, M., Smith, S., 2001. The role of registration in functional magnetic resonance imaging. In: Hajnal, J.V., Hill, D.L.G., Hawkes, D.J. (Eds.), Medical Image Registration. CRC Press, New York, pp. 183 – 198.

Jokisch D, Roser P, Juckel G, Daum I, Bellebaum C. (2014). Impairments in Learning by Monetary Rewards and Alcohol-Associated Rewards in Detoxified Alcoholic Patients. Alcohol Clin Exp Res. Jun 13.

Klein, Stephen B. (2012). Learning : principles and applications. Thousand Oaks, Calif. : Sage Publications, Inc, 2012.

Kober, T., Marques, J.P., Gruetter, R., Krueger, G. (2011). Head motion detection using FID

Koush Y, Zvyagintsev M, Dyck M, Mathiak KA, Mathiak K. (2012). Signal quality and Bayesian signal processing in neurofeedback based on real-time fMRI. Neuroimage. Jan 2;59(1):478-89.

Lee TY, Su HR, Lai SH, chiun Chang T. Compensation of motion artifacts in mri via graph-based optimization. In Computer Vision and Pattern Recognition, 2009. CVPR 2009. IEEE Conference on. 2192–2199.

Lin W, Song H. Extrapolation and correlation (EX- TRACT): a new method for motion compensation in MRI. IEEE Transactions on Medical Imaging 2009; 28:82–93.

Lin W, Wehrli F, Song H. Correcting bulk in-plane motion artifacts in MRI using the point spread function. IEEE Transactions on Medical Imaging 2005; 24:1170–1176.

Maclaren J, Armstong BS, Barrows RT, Danishad KA, Ernst T. Foster CL, Gumus K, Herbst M, Kadashevich IY, Kusik TP, Li Q, Lovell-Smith C, Prieto T, Schulze P, Speck O, Stucht D, Zaitsev M. Measurement of microscopic head motion during brain imaging. In Proceedings of the 20th Scientific Meeting ISMRM, Montreal, Canada, 2011. p. 144.

Mathiak, K., Posse, S. (2001). Evaluation of motion and realignment for functional magnetic resonance imaging in real time. Magn. Reson. Med. 45, 167–171.

McConnell MV, Khasgiwala VC, Savord BJ, Chen MH, Chuang ML, Manning WJ, Edelman RR. Prospective adaptive navigator correction for breath-hold MR coronary angiography. Magn Reson Med 1997;37: 148–152..

Noll DC, Schneider W. Theory, simulation and compensation of physiological motion artifacts in functional MRI. In: Proceedings of IEEE International Conference on Image Processing, Austin, Texas, 1994. p40.

Oakes TR, Johnstone T, Ores Walsh KS, Greischar LL, Alexander AL, Fox AS, Davidson RJ. (2005). Comparison of fMRI motion correction software tools. Neuroimage. Nov 15;28(3):529-43.

Ooi MB, Krueger S, Thomas WJ, Swaminathan SV, Brown TR. Prospective real-time correction for arbitrary head motion using active markers. Magn Reson Med 2009;62:943–954.

Ooi, M. B., Krueger, S., Thomas, W. J., Swaminathan, S. V., & Brown, T. R. (2009). Prospective real-time correction for arbitrary head motion using active markers. Magnetic Resonance in Medicine, 62(4), 943-954.

Qin L, van Gelderen P, Derbyshire JA, Jin F, Lee J, de Zwart JA, Tao Y, Duyn JH. Prospective head-movement correction for high-resolution MRI using an in-bore optical tracking system. Magnetic Resonance in Medicine 2009; 62:924–934.

Raygor R. *The Science of Psychology*, New York; McGraw-Hill 2005.

Ruiz, S., Buyukturkoglu, K., Rana, M., Birbaumer, N., Sitaram, R. (2013). Real-time fMRI brain computer interfaces: Self-regulation of single brain regions to networks . Biol Psychol. 2014 Jan;95:4-20.

Sakurai Y, Song K, Tachibana S, Takahashi S. (2014). Volitional enhancement of firing synchrony and oscillation by neuronal operant conditioning: interaction with neurorehabilitation and brain-machine interface. Front Syst Neurosci. Feb 6;8:11. doi: 10.3389/fnsys.2014.00011.

Schacter DL, Gilbert DT, Wegner DM. Psychology (2nd Edition). New York: Worth; 2011

Schulz J, Siegert T, Reimer E, Zaitsev M, Maclaren J, Herbst M, Turner R. First embedded in-bore system for fast optical prospective head motion-correction in MRI. In Proceedings of the 28th Annual Scientific Meeting of the ESMRMB, Leipzig, Germany, 2011. p. 369.

Skinner, B.F. (1974). About Behaviorism. New York: Alfred A. Knopf.

Sulzer J, Haller S, Scharnowski F, Weiskopf N, Birbaumer N, Blefari ML, Bruehl AB, Cohen LG, DeCharms RC, Gassert R, Goebel R, Herwig U, LaConte S, Linden D, Luft A, Seifritz E, Sitaram R. (2013). Real-time fMRI neurofeedback: progress and challenges. Neuroimage. Aug 1;76:386-99.

Thacker, N.A., Burton, E., Lacey, A.J., Jackson, A., 1999. The effects of motion on parametric fMRI analysis techniques. Physiol. Meas. 20, 251 – 263.

Thesen S, Heid O, Mueller E, Schad LR. Prospective acquisition cor- rection for head motion with image-based tracking for real-time fMRI. Magn Reson Med 2000; 44:457–463.

Tisdall MD, Hess AT, Reuter M, Meintjes EM, Fischl B, van der Kouwe AJW. Volumetric navigators for prospective motion correction and selective reacquisition in neuroanatomical mri. Magnetic Resonance in Medicine 2012; 68:389–399.

van der Kouwe, A.J., Benner, T., Dale, A.M. (2006). Real-time rigid body motion correction and shimming using cloverleaf navigators. Magn. Reson. Med. 56, 1019–1032.

Ward, H.A., Riederer, S.J., Grimm, R.C., Ehman, R.L., Felmlee, J.P., Jack Jr., C.R., 2000. Prospective multiaxial motion correction for fMRI. Magn. Reson. Med. 43, 459–469.

Weinhandl JT, Armstrong BS, Kusik TP, Barrows RT, O’Connor KM. Validation of a single camera three-dimensional motion tracking system. J Biomech 2010;43:1437–1440.

Weiskopf, N., Sitaram, R., Josephs, O., Veit, R., Scharnowski, F., Goebel, R., Birbaumer, N., Deichmann, R., Mathiak, K. (2007). Real-time functional magnetic resonance imaging: methods and applications. Magn. Reson. Imaging 25, 989–1003.

Welch E, Manduca A, Grimm R, Ward H, Jack C. Spherical navigator echoes for full 3-d rigid body motion measurement in MRI. In Medical Image Computing and Computer-Assisted Intervention–MICCAI 2001.

Welch EB, Manduca A, Grimm RC, Ward HA, Jack Jr CR. Spherical navigator echoes for full 3D rigid body motion measurement in MRI. Magn Reson Med 2002;47:32–41.

White N, Roddey C, Shankaranarayanan A, Han E, Rettmann D, Santos J, Kuperman J, Dale A. Promo: Real-time prospective motion correction in mri using image- based tracking. Magnetic Resonance in Medicine 2010; 63:91–105.

Zaitsev M, Dold C, Sakas G, Hennig J, Speck O. Magnetic resonance imaging of freely moving objects: prospective real-time motion correction using an external optical motion tracking system. Neuroimage 2006;31:1038–1050.

Figures and Tables

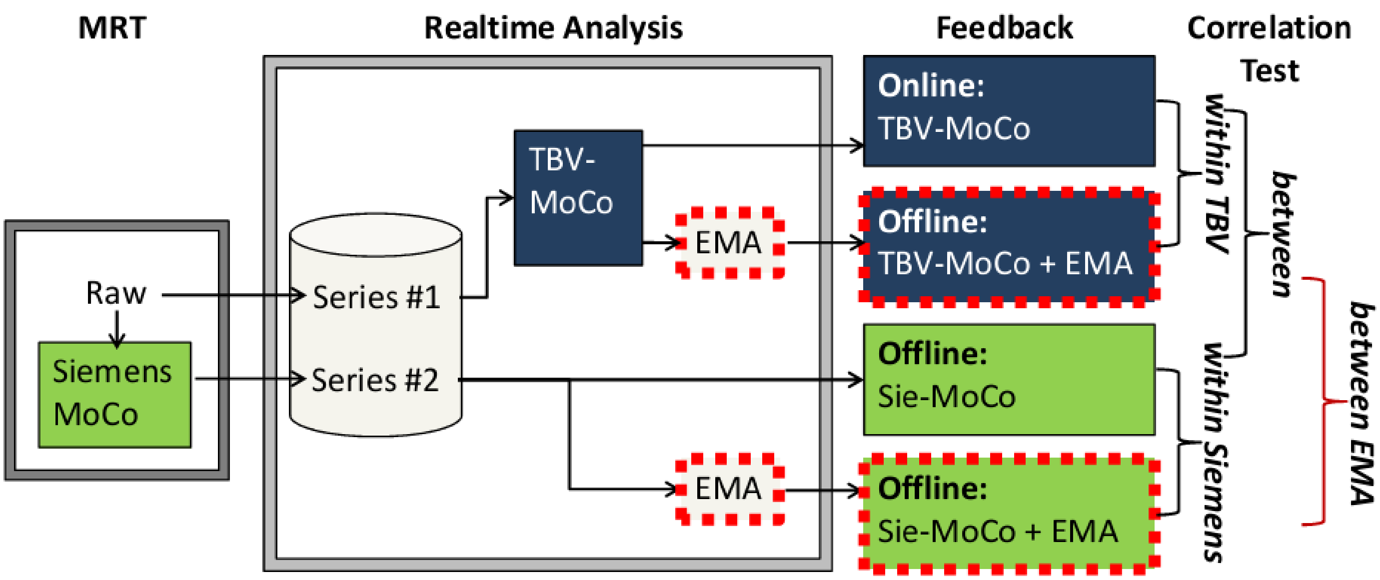

Figure 1: Setup of the experiment. Raw data from scanner is saved as series #1 and motion corrected as series #2. Realtime analysis includes TBV motion correction for series #1. In correlation tests „within“ refers to correlations within one algorithm and „between“ to correlations between the two motion correction algorithms.

Table1: Subject data and ROI sizes

Subject	age (y)	sex	ROI1 (voxel)	ROI2 (voxel)	ROI3 (voxel)
1	27	m	14	10	35
2	34	f	12	17	77
3	27	m	66	66	56

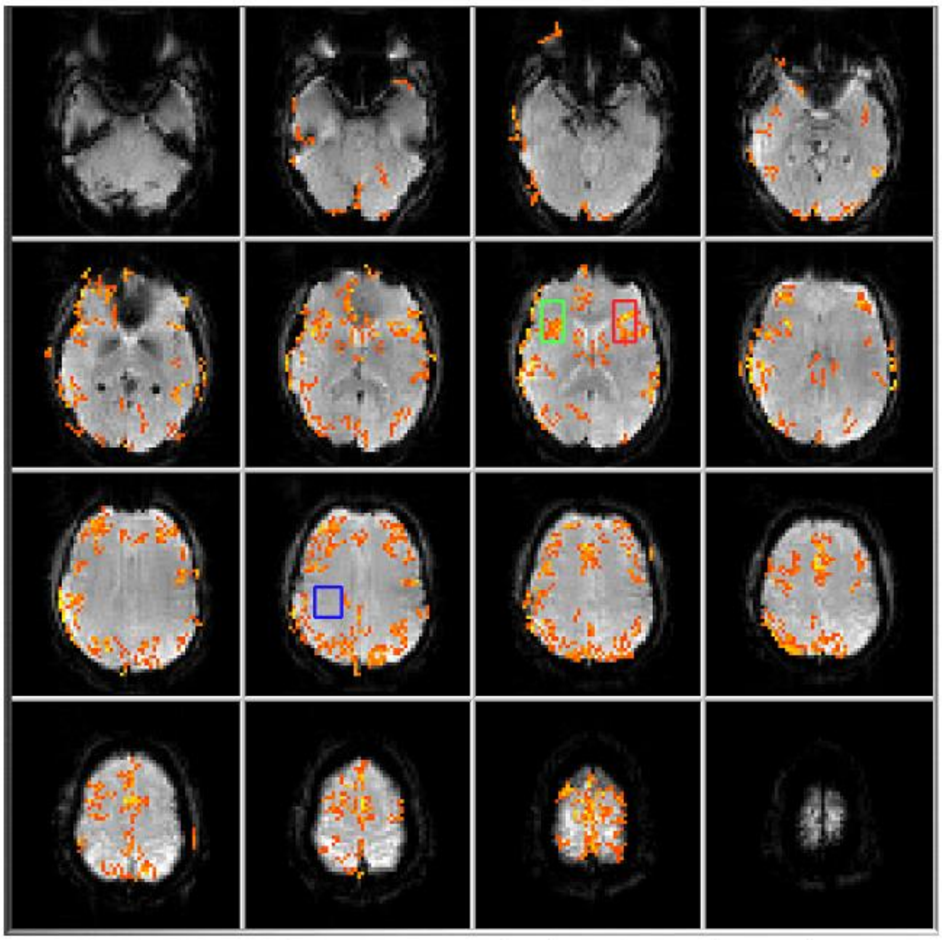

Figure 2: Regions of interest. ROI1 (red) and ROI2 (green) are active regions. ROI3 (blue) defines a control region.

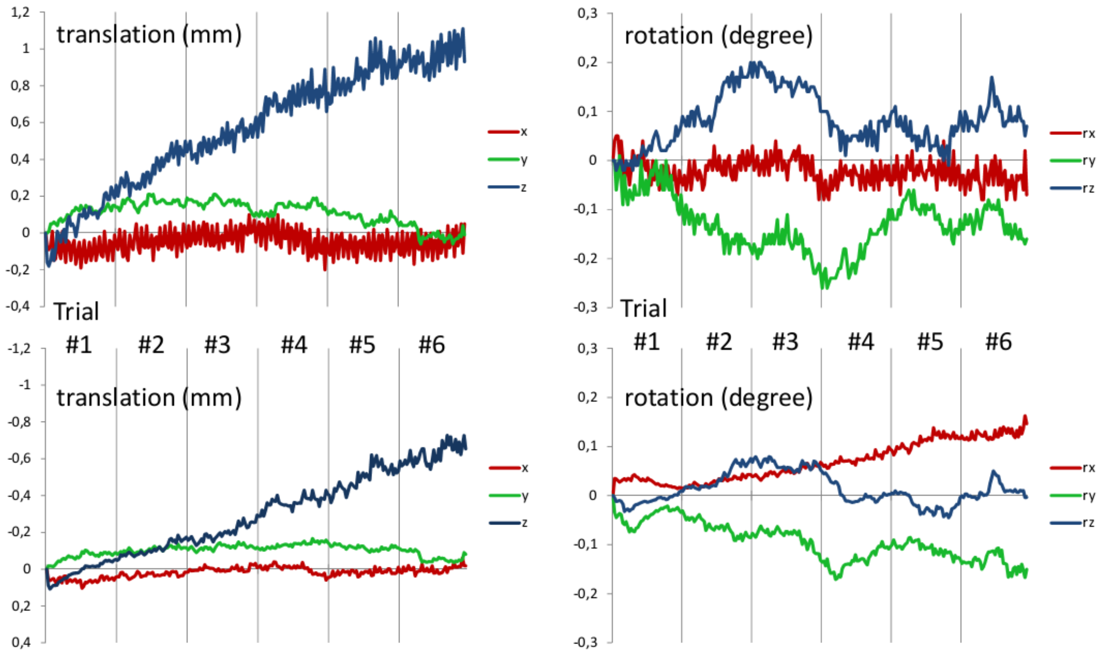

Figure 3a: Timeplots of motion correction parameters. In all four plots the abscissa represents 360 seconds. Top row: Siemens, bottom row: TBV. Left side: translation parameters, x, y and z. Right side: rotation parameters, rx, ry and rz. To correct for the different notation of TBV and Siemens MoCo parameters, the ordinate of the plot in the lower left is flipped.

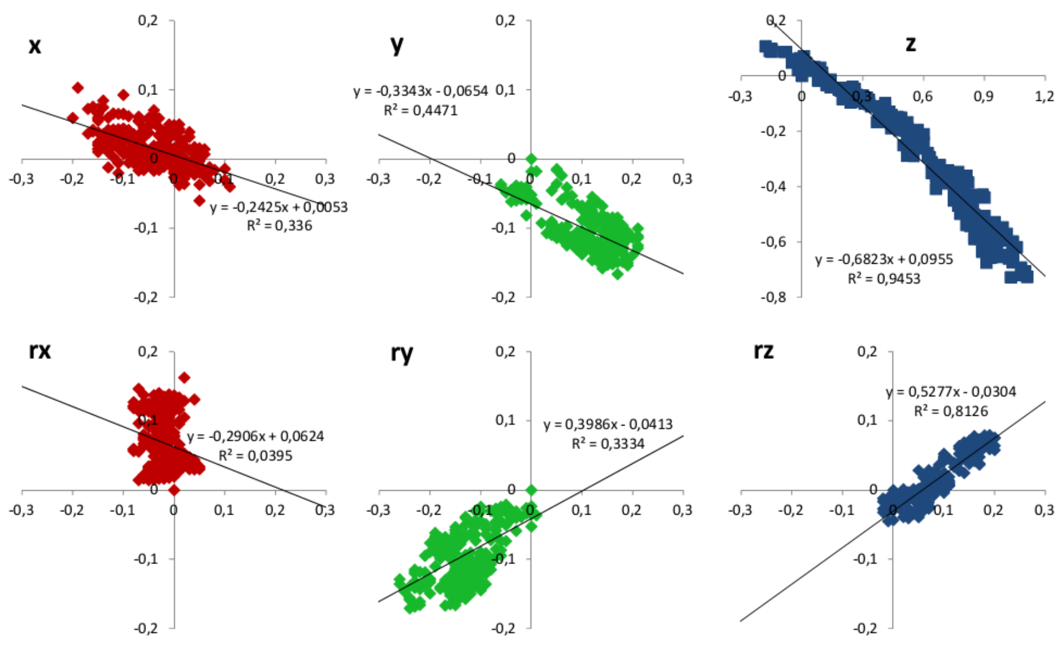

Figure 3b: Correlation of the motion correction parameters .
Top: Translations x, y, z. Bottom: rotations rx, ry, rz

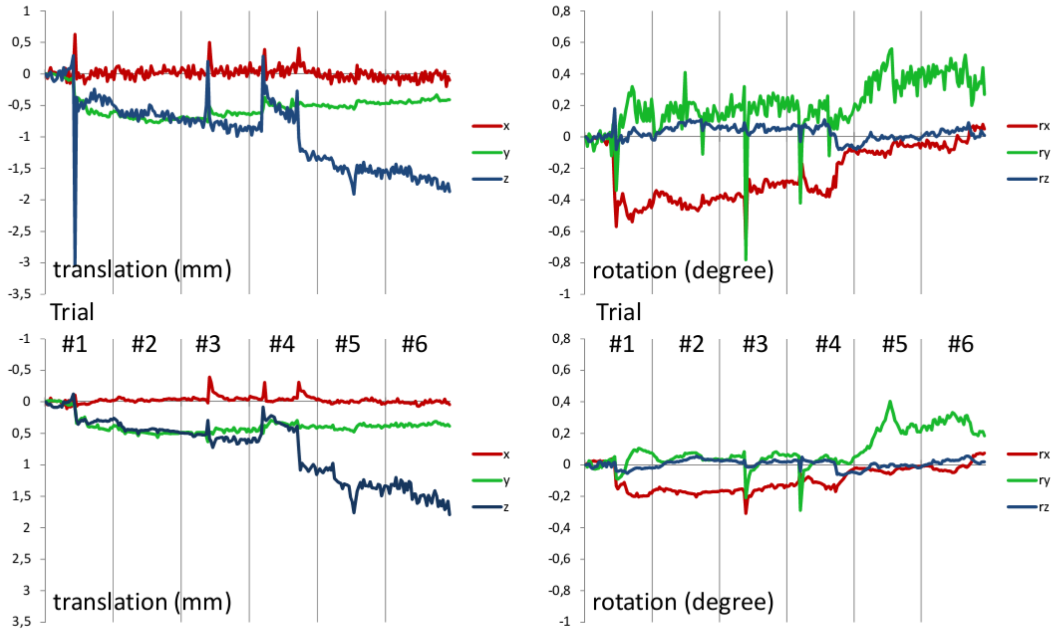

Figure 4a: Timeplots of motion correction parameters. In all four plots the abscissa represents 360 seconds. Top row: Siemens, bottom row: TBV. Left side: translation parameters, x, y and z. Right side: rotation parameters, rx, ry and rz. To correct for the different notation of TBV and Siemens MoCo parameters, the ordinate of the plot in the lower left is flipped.

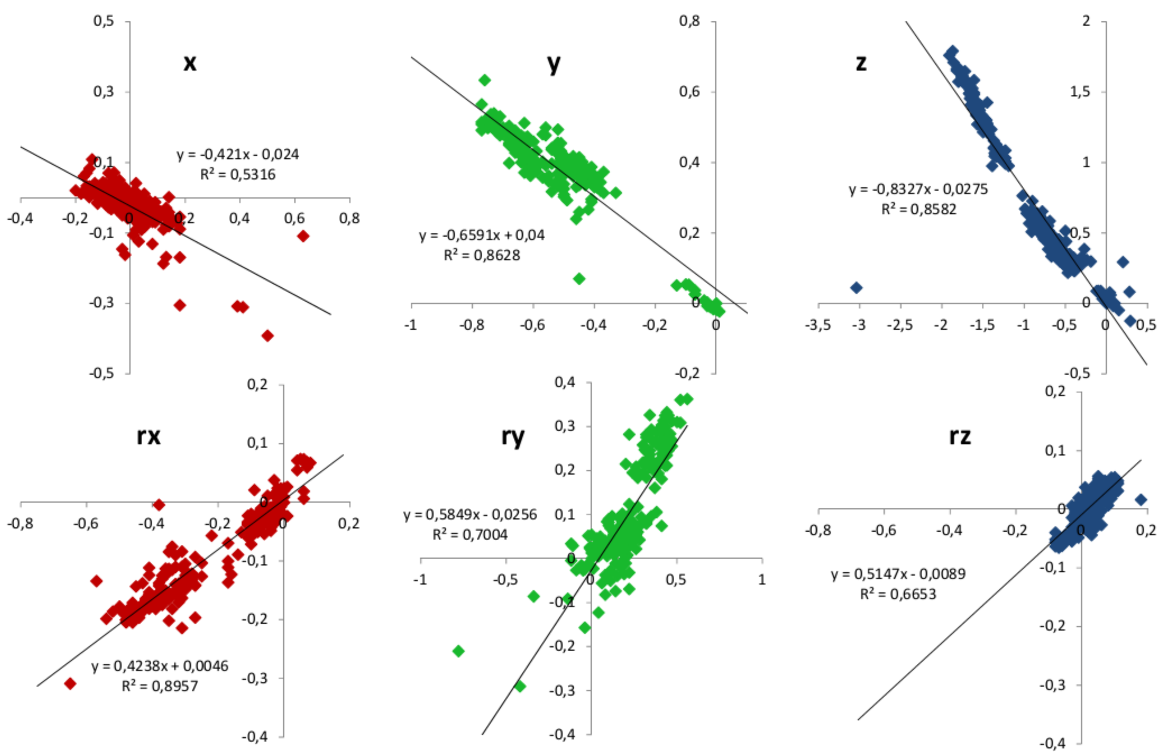

Figure 4b: Correlation of the motion correction parameters .
Top: Translations x, y, z. Bottom: rotations rx, ry, rz

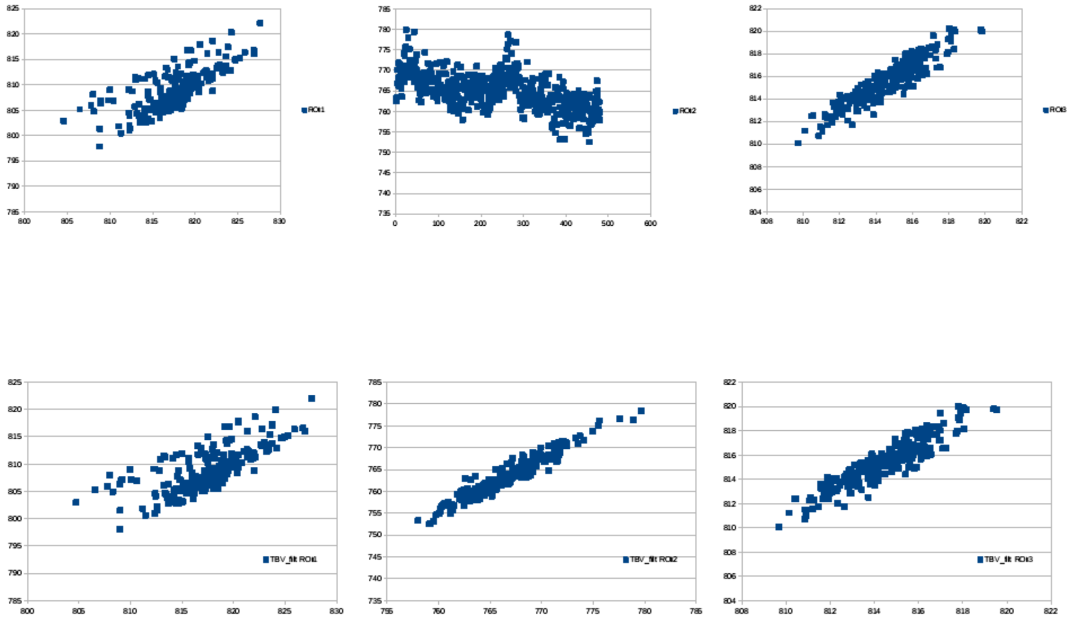

Figure 5: Correlations between ROIs calculated from TBV MoCo data and Siemens MoCo data Subject 1, first session, fifth run. Top: unfiltered data. Bottom: filtered data.

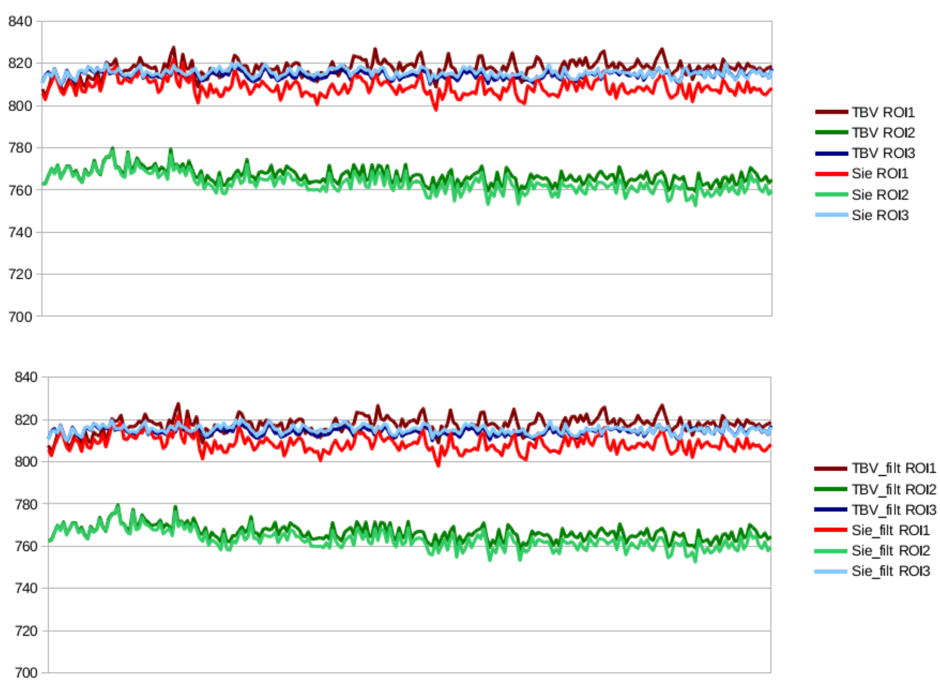

Figure 6: Timeplots of ROI averages for subject 1, first session, fifth run. Top: unfiltered data. Bottom: filtered data. TBV = TurboBrainVoyager motion correction, Sie = Siemens MoCo.

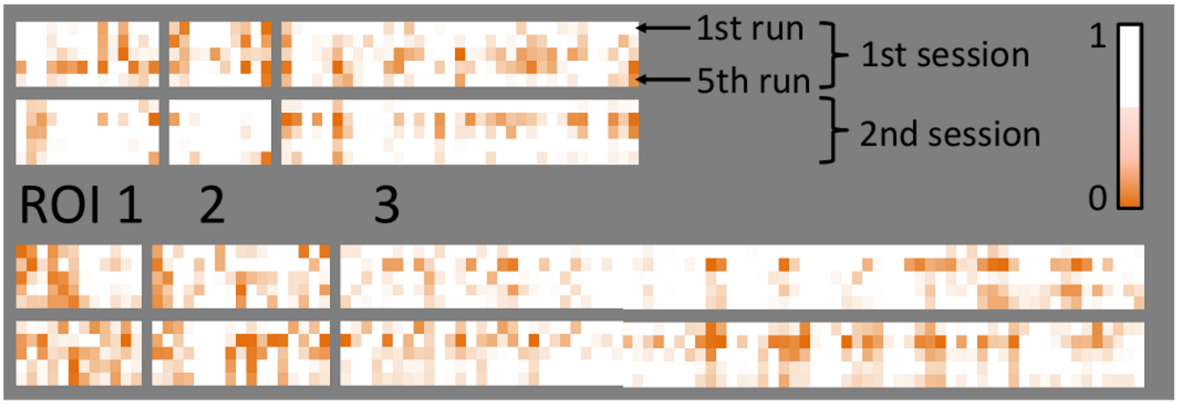

Figure 7a: r² of voxel values between TBV- and Siemens motion corrected images. All ROIs, subjects 1 (top) and 2 (bottom), first and second session, all runs. Voxels are lined up for the runs. Low values are displayed in red.

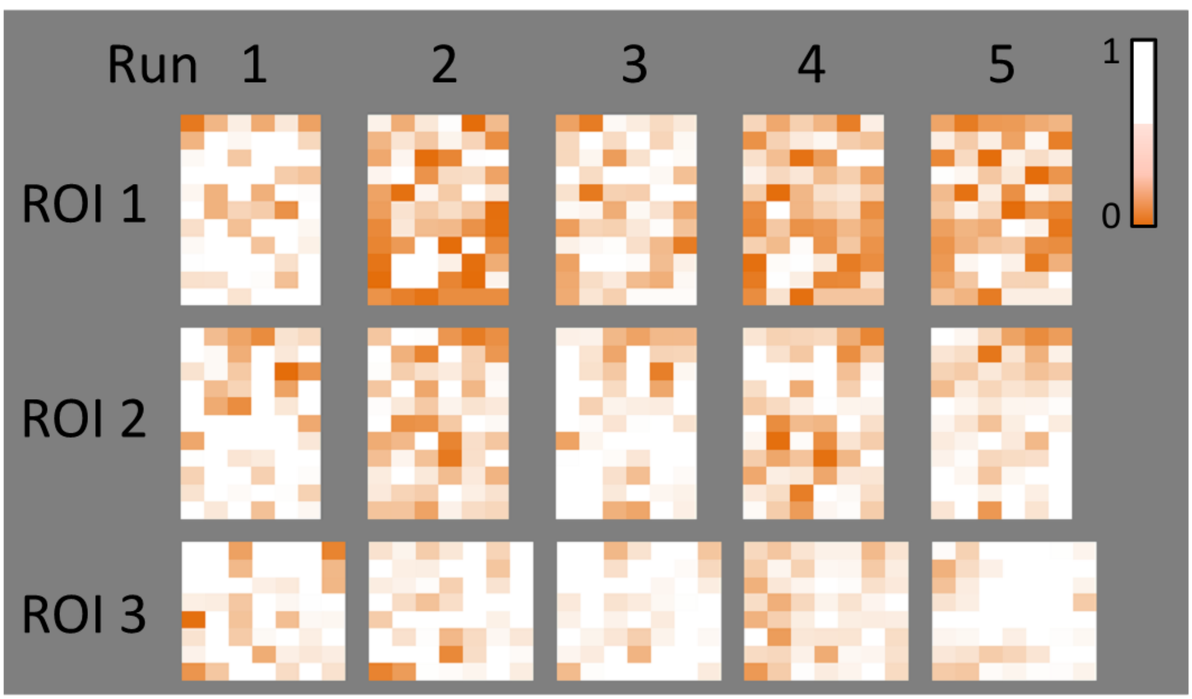

Figure 7b: Subject 3, session 3, ROIs visualized in original shape. Reduced correlation is not restricted to voxels along the edges.

Table 2: Correlations of the motion correction (MoCo) parameters from TBV and Siemens (six degrees of freedom) and of the feedback parameters derived from the motion corrected data. Displayed is R^2. Values below 0.6 are highlighted in orange and in the range 0.8 to 0.6 in light orange. Each row represents one run. The "between" columns refer to the correlations between the MoCo-pipelines. "Within" shows the correlation between original data and filtered data within one MoCo-pipeline (Figure 1). Values close to 1 in the "within" columns indicate little effect of the filter on the data.

			Motion correction parameters						unfiltered	EMA-filter			Outlier removal 1			Outlier removal 2				
			Translation			Rotation			Between	Between	Within		Between	Within		Between	Within		Nr. of rejected vol.	
Subj	Sess	Run	x	y	z	rx	ry	rz			TBV	Siemens		TBV	Siemens		TBV	Siemens	TBV	Siemens
1	1	1	0,83	0,85	0,97	**0,10**	0,96	**0,58**	0,85	0,85	1,000	1,000	**0,09**	**0,20**	0,85	0,80	0,92	0,94	12	9
		2	0,92	**0,57**	0,99	**0,00**	0,99	0,96	**0,76**	**0,76**	1,000	1,000	0,81	**0,57**	0,82	0,83	0,96	0,99	10	13
		3	0,95	0,88	0,99	**0,01**	0,98	0,95	0,82	0,82	1,000	1,000	**0,76**	0,85	**0,78**	**0,71**	0,99	0,98	15	10
		4	0,93	0,91	0,98	**0,33**	0,97	0,97	**0,21**	**0,21**	1,000	1,000	**0,61**	0,96	**0,22**	**0,15**	0,95	0,85	18	15
		5	**0,34**	**0,45**	0,95	**0,04**	**0,33**	0,81	**0,75**	**0,75**	1,000	1,000	**0,63**	**0,70**	**0,80**	**0,74**	1,00	0,99	11	8
	2	1	**0,64**	0,80	**0,64**	**0,67**	**0,44**	**0,33**	0,92	0,92	1,000	1,000	0,92	0,95	0,95	0,84	0,98	0,92	8	5
		2	0,95	0,96	**0,67**	**0,53**	0,93	**0,72**	**0,64**	**0,63**	0,997	0,999	0,89	**0,63**	0,86	**0,51**	**0,77**	**0,72**	13	6
		3	0,91	**0,53**	**0,26**	**0,45**	0,83	0,86	**0,71**	**0,70**	1,000	1,000	**0,13**	**0,57**	**0,31**	**0,67**	**0,79**	**0,65**	5	5
		4	**0,63**	**0,76**	**0,55**	**0,47**	**0,74**	0,85	0,84	0,85	1,000	1,000	**0,57**	**0,65**	**0,38**	0,83	0,98	0,97	7	7
		5	**0,49**	0,96	**0,79**	**0,71**	0,94	0,94	0,95	0,95	1,000	1,000	**0,57**	**0,27**	**0,72**	0,85	0,98	0,93	6	7
2	1	1	**0,79**	0,97	0,96	0,87	0,93	0,89	0,93	0,93	1,000	1,000	**0,65**	0,89	**0,80**	0,97	0,98	0,99	5	6
		2	**0,31**	0,93	0,96	0,89	0,97	0,92	0,92	0,92	1,000	1,000	0,96	0,82	0,87	0,93	0,97	0,98	9	3
		3	0,96	**0,75**	**0,53**	**0,48**	**0,68**	0,95	**0,45**	**0,45**	1,000	1,000	**0,22**	**0,05**	**0,53**	**0,58**	**0,76**	0,84	12	8
		4	0,92	0,95	0,85	**0,55**	0,84	0,88	0,90	0,90	1,000	1,000	**0,42**	**0,32**	**0,05**	0,93	0,82	**0,80**	11	11
		5	0,95	0,88	**0,71**	0,86	0,84	0,89	**0,79**	**0,78**	1,000	1,000	**0,64**	**0,75**	0,86	**0,71**	0,96	0,99	5	6
	2	1	0,98	0,95	**0,40**	**0,65**	0,86	0,89	**0,03**	**0,03**	1,000	1,000	**0,03**	**0,57**	**0,30**	**0,06**	0,99	0,96	5	5
		2	**0,59**	0,99	0,94	0,96	**0,74**	0,98	0,96	0,96	1,000	1,000	**0,79**	0,86	0,82	0,91	0,99	0,98	12	10
		3	0,85	**0,75**	0,82	0,90	0,94	0,87	**0,77**	**0,77**	1,000	1,000	**0,46**	**0,50**	**0,73**	0,81	0,97	0,93	5	9
		4	**0,64**	0,94	**0,70**	0,84	0,86	0,92	**0,38**	**0,38**	1,000	1,000	**0,14**	**0,78**	**0,29**	**0,24**	**0,79**	0,89	8	8
		5	0,85	0,94	0,86	**0,40**	**0,71**	**0,73**	**0,21**	**0,20**	1,000	1,000	**0,60**	0,96	**0,69**	**0,05**	**0,69**	**0,65**	9	9
3	1	1	**0,77**	0,99	0,95	0,82	0,92	0,98	**0,00**	**0,00**	1,000	1,000	**0,10**	**0,80**	0,99	**0,02**	0,93	**0,78**	8	23
		2	**0,60**	0,90	0,83	**0,65**	0,82	0,95	**0,76**	**0,77**	1,000	1,000	**0,69**	**0,69**	0,95	0,90	0,81	0,91	11	13
		3	**0,76**	0,91	0,88	**0,55**	**0,76**	**0,60**	0,83	0,83	1,000	1,000	**0,66**	0,87	0,99	0,86	0,97	0,98	22	22
		4	**0,71**	0,92	0,88	**0,77**	0,80	0,94	**0,27**	**0,27**	1,000	1,000	**0,15**	**0,63**	**0,60**	**0,26**	**0,29**	**0,69**	10	11
		5	**0,66**	0,92	0,87	0,83	0,84	0,90	**0,20**	**0,20**	1,000	1,000	**0,16**	0,84	0,91	**0,45**	0,83	0,95	9	14
	2	1	0,94	0,95	0,86	**0,68**	**0,58**	**0,64**	0,94	0,94	1,000	1,000	0,97	0,88	**0,72**	0,88	0,94	**0,72**	14	19
		2	**0,74**	0,94	0,92	**0,68**	0,85	**0,04**	0,99	0,99	1,000	1,000	**0,75**	**0,68**	**0,71**	0,98	**0,74**	0,88	24	23
		3	**0,77**	0,80	0,94	**0,49**	**0,73**	**0,69**	**0,43**	**0,43**	1,000	1,000	**0,05**	**0,56**	0,93	**0,72**	**0,61**	**0,63**	9	17
		4	**0,68**	0,83	0,88	**0,69**	**0,69**	**0,59**	0,92	0,92	1,000	1,000	**0,69**	**0,00**	**0,00**	0,84	**0,55**	0,81	9	13
		5	**0,72**	0,93	**0,73**	**0,74**	**0,59**	0,88	0,92	0,92	1,000	1,000	0,95	0,84	0,89	0,90	0,87	0,94	9	19
	3	1	**0,80**	0,98	0,95	**0,60**	0,86	**0,77**	0,96	0,96	1,000	1,000	0,91	0,96	1,00	0,96	0,91	0,95	11	13
		2	**0,53**	0,86	0,86	0,90	**0,70**	**0,67**	**0,76**	**0,77**	1,000	1,000	**0,33**	**0,23**	0,92	0,80	0,92	0,94	24	24
		3	0,87	0,94	0,94	**0,76**	**0,68**	**0,76**	**0,67**	**0,68**	1,000	1,000	**0,55**	**0,68**	0,83	**0,58**	0,93	0,83	13	18
		4	0,93	0,87	0,87	**0,68**	0,83	**0,64**	0,84	0,84	1,000	1,000	0,91	0,88	0,98	**0,78**	0,83	0,99	16	21
		5	0,81	0,93	0,91	**0,62**	**0,74**	0,81	**0,54**	**0,54**	1,000	1,000	**0,61**	0,97	0,94	**0,60**	0,99	0,99	10	22